Chapter 3

DAP/alginate Based Nanosilver Composite Hybrid Gel Beads for Topical Drug Delivery Applications

3.1 Introduction

Microbial infection is one of the most common diseases in the present era and there are many antimicrobial agents available for its treatment. The inappropriate use of antibiotics results in resistance genes against antibiotics.[1-3] Antibacterial resistance is a multiplex mechanism whose diagnosis depends on the bacterial strains, resistance mechanisms and individual.[4] Antibacterial resistance to conventional antibiotics, however, has emerged as one of the major global public health threats facing humanity[5] which reinforce the requirement for innovation, prevention, diagnosis, keeping an eye on antibiotic consumption and their misuse. Thus supervision of antibiotics pharmacodynamics and pharmacokinetics is necessary to reduce the toxicity and threat of progressing antibacterial resistance.[6] To tackle the trouble of resistance, it is necessary to alter the conventions of antibacterial use[7] and their administration should be suggested only when other treatments are not working and therefore, to overcome, the problem of resistance, some non-traditional antibacterial agents are developing great interest.[2] Along with there is a need of cooperative endeavour of intellectual networks and governments to fight against multidrug resistant bacteria. Nanoparticles (NPs) received researchers attention because of having small size (1–100 nm), increased reactivity, unique properties, ability to penetrate the skin, large surface area and various applications in agriculture, modern science and in pharmaceutical sciences and are considered to be good alternative to solve the threat of microbial multidrug resistance.[8] A various kinds of metallic nanoparticles of titanium, zinc, magnesium, gold, copper and silver have been reported.[9-11] Silver nanoparticles (AgNPs) are more attractive because of having great applications in different scientific fields like optics, optoelectronics and pharmaceutical sciences for drug delivery applications, gene

therapy, therapeutic agents and biosensors etc.[12-15] AgNPs also have been appraised for marvellous applications like on patients for prostheses, bone cement, trauma, protective clothing and dental implants,[16-17] etc. The strong antimicrobial, anticancer, antibiofilm and anti-inflammatory activities of AgNPs have been already reported[11,18] and therefore their use has been known to be commercial in several industries for products, like footwear, hand gel, wound dressings, plastics, paints, cosmetics and medical catheter coverings, etc.[19] Alongwith AgNPs have strong bactericidal and sterilization effect against numerous drug-resistant pathogenic microbe.[20] It is reported that AgNPs can interact physically with the surface of the cell of various bacteria and can spoil cell memberanes resulting to change in structure and make the bacteria more permeable.[21,22] A numerous studies reported that the activty of AgNPs depends on their size.[23,24] AgNPs with smaller dmensions have greater antibacerial actvity and it is considered that a fixed amount of silver cations is released from the AgNPs on dissolving in water or during penetrating the cells. It is reported that the NPs have higher antimicrobial activities than the free silver ions. In addition the free ions and NPs collectively produce antimicrobial effect of broad range with more strength. Moreover the microbial resistance to AgNPs is found to be rare because of manifold bactericidal mechanism.[25] Ag ions can interact with a number of electron rich fuctional moities like phosphates, imidazoles, thiols, indols and hydroxyls. AgNPs with small dimensions and Ag ions can easily penetrate the microbial body by demaging the intracellular structures and may be resulted out the denaturation of ribosomes by inhibition of protein synthesis, as well as, can cause the bockage of transcription and translation by bacterial cell genetic material.[26-28] The effect of the concentration of the AgNPs on antibacterial activity depends on the class of bacteria.[29] Definitely, *Vibrio cholera* and *Pseudomonas*

aeruginosa were found to be more resistant than *Salmonella typhi* and *E. coli*, but at concentrations higher than 75 μg/mL, the growth of bacteria was completely stopped.[30] In this point of view, Kim *et al.*[31] reported that AgNPs shows good antibacterial activity against *E. coli* even at low concentration of NPs while inhibitory effect is slow against *S. aureus*.[23] It has been recommended that AgNPs can also effect the bacterial replication processes by interacting.[32] The factors affecting the activity of AgNPs (UV radiations, size, shape and concentration) should be kept in mind during their preparation for clinical use.[33]

Silver nanoparticles (AgNPs) show broad spectrum properties as anti-microbial agents, anti-biofilm agents, drug delivery agents, optoelectronic platforms and imaging probes. In addition they are known to be a superior alternative to conventional antibiotics in view of unique mechanisms of action which prevents the generation of bacterial resistance.[34] The various physical and chemical techniques have been broadly used for the nanoparticles synthesis, but unfortunately, these techniques have some limitations like yeilding of environmentally unfriendly fatal byproducts, hazardous chemicals use and great expense.[35] To overcome these drawbacks of physical and chemical tecniques, Different polymers have also been used for the coating of AgNPs, which provides stability, commercial, ecofriendly and also reduces the toxicity of NPs tothe microbial host.[36,37] The AgNPs loaded hydrogels were reported by many authors because of its vast applications associated with drug development processes[5,38-42] and are still in progress towards the development of mild and efficient method of Ag nanocomposite gels.[43-44] Accordingly, the antibacterial gelling agents are good choices for the silver nanocomposites with enhanced antimicrobial efficacy of AgNPs for the formation of gels and hybrid gels.[45] Recently we synthesized a variety of simple low molecular mass

gelators starting from 2,6-diaminopyridine (DAP) for drug incorporation and release study.[46]

The various physical and chemical techniques have been broadly used for the nanoparticles synthesis, but unfortunately, these techniques have some limitations like yeilding of environmentally unfriendly fatal byproducts, hazardous chemicals use and great expense.[35] To overcome these drawbacks of physical and chemical tecniques, Different polymers have also been used for the coating of AgNPs, which provides stability, commercial, ecofriendly and also reduces the toxicity of NPs to the microbial host.[36,37] The AgNPs loaded hydrogels were reported by many authors because of its vast applications associated with drug development processes[5,38-42] and are still in progress towards the development of mild and efficient method of Ag nanocomposite gels.[44,47] Therefore, the gels formed by the gelling agents showing antibacterial activity are of great interest to increase the antibacterial efficacy of AgNPs in optimized and synergetic action toward the synthesis of ideal gel.[45]

Organogels formed by self-assembled low molecular weight gelators have attracted the attention of the scientific community since the late 1990s[48,49] because of their wide variety of applications such as self-healing materials,[50] fat-free food products,[51] pollutant removal,[52] drug delivery systems,[53] analysis and purification-related systems.[54] They are more efficient over aqueous solution of drugs for topical applications because of their high viscosity and microbial contamination resistivity.[55] During recent years, low molecular weight gelators (LMWGs) have become a point of attraction of researchers due to their various applications in optoelectronics, environmental remediation, energy storage, pharmaceuticals and drug delivery.[56] The specific applications of gels can be

optimized by physical and chemical interactions within LMWG self-assemblies, however, it is challenging to provide self-assembled gels with craved structures and shapes that may offer new prospective for low molecular weight gelators.[57] Usually the gelswith appropriate structures and shapes can act as a carrier for drug delivery.[58] Several techniques techniques have been developed to control the shape and structure of the gelation, including 3D printing,[59] moulding and photopatterning,[60] surface mediated processes[61] and electrochemistry.[62] A number of methods have also been used to obtain shape controlled resolution[63] but there are only limited reports available in the literature where gels are drafted as spherical particles. The formation of gel microspheres was reported by Miravet and co-workers by dropwise addition of gelator-DMSO solution in an anti-solvent.[64]

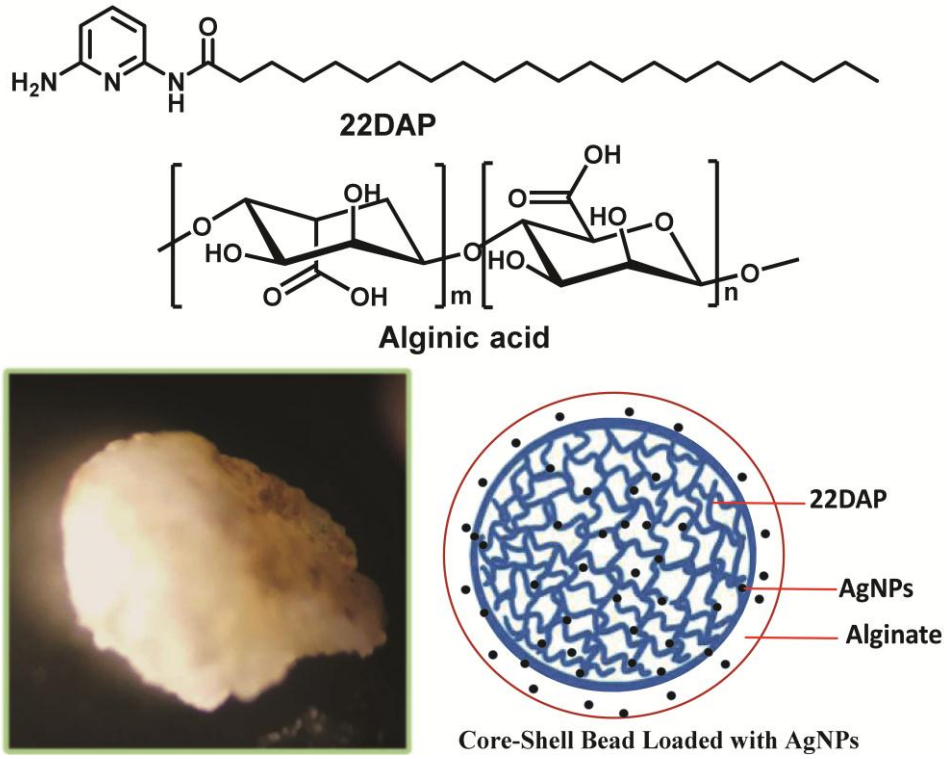

Figure 3.1. Structures of **22DAP** and alginic acid, microscopic image (left) of hybrid **22DAP**/alginate gel bead loaded with AgNPs and graphic diagram (right) of an AgNPs-loaded core–shell gel bead.

Buerkle and Rowan[65] defined mainly three types of multi-component gels based on LMW gelators: *i) neither of the two components has the ability to form gels individually, but can self-assemble into a sample-spanning network of non-covalent interactions with the other molecular component. ii) a two-component gel where both gelators can interact to form co-fibers within their individual networks; iii)* a gelator and a non-gelling ingredient, which act in some way to alter the function of the gel. Of these types, most of the second type of hybrid gel is of specific interest among researchers, which can be formed by combining LMWGs and polymer gelators, in which polymeric gel network can accelerate the nature of LMWGs[65,66] and help to control the shape and structure.[57]

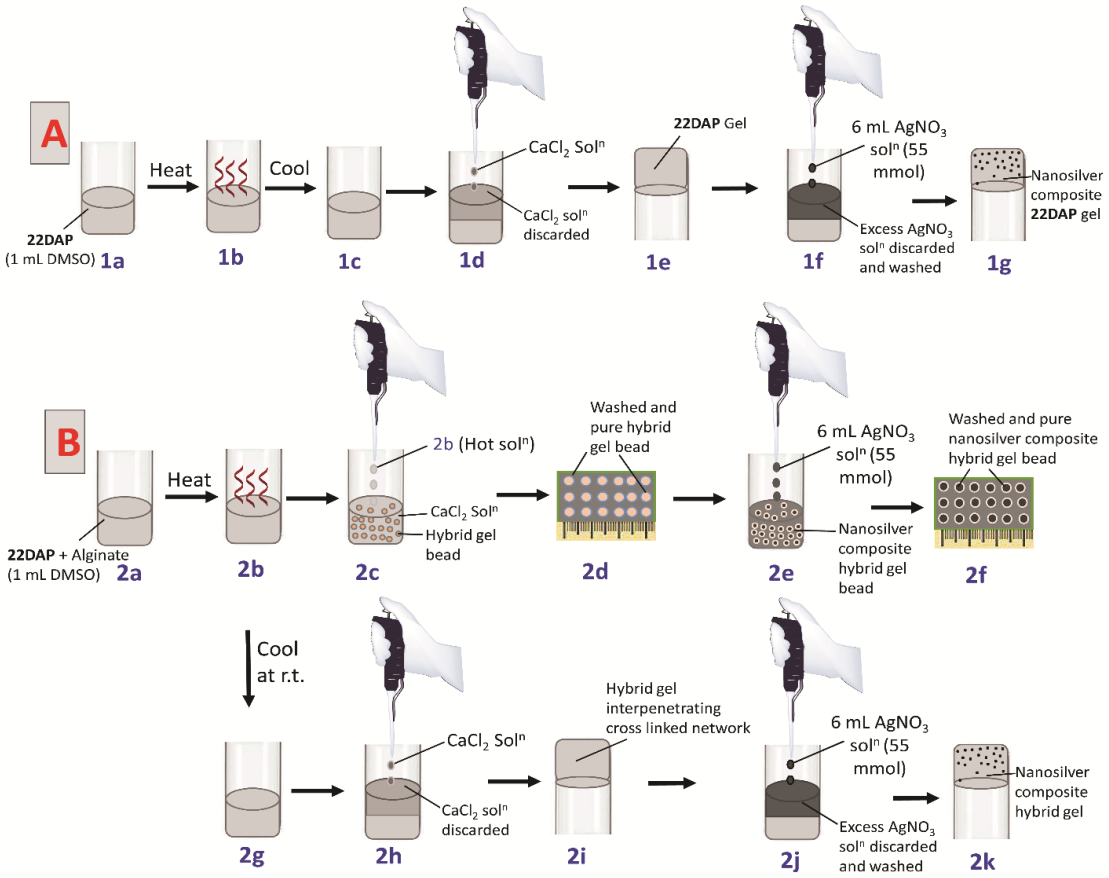

For figure caption (Please see next page)

Figure 3.2. Schematic representation for the preparation of nanosilver composite single component **22DAP** gel, **22DAP**/alginate hybrid gel bead and multicomponent hybrid gel[44,70]; **A: 1a)** 10 mg **22DAP** is suspended in DMSO (1 mL); **1b)** The suspension was heated until complete dissolution of **22DAP**; **1c)** The hot solution was cooled at r.t.; **1d)** An aqueous solution of $CaCl_2$ (5%, 2 mL) was then added on the top of gel to diffuse in; **1e)** A single component **22DAP** gel was prepared as a control; **1f)** A 55 mmol $AgNO_3$ solution (6 mL) was added on the top of single component **22DAP** gel and left for 3 days then $AgNO_3$ solution was discarded carefully with the help of pipette and further washed with water for three times; **1g)** Nanosilver composite single component **22DAP** gel; **B: 2a**) **22DAP** and alginate were suspended in DMSO (1 mL); **2b)** The suspension was heated until complete dissolution of **22DAP** and alginate; **2c)** The hot solution of 2b was added drop wise into another vial containing 5% $CalCl_2$ solution for the formation of core-shell shaped hybrid gel beads; **2d)** $CalCl_2$ solution was removed with the help of pipette and washed with water (three times) to get pure hybrid gel beads; **2e)** A 55 mmol $AgNO_3$ solution (6 mL) was added to the vial containing pure hybrid gel beads and left for 3 days then $AgNO_3$ solution was discarded carefully with the help of pipette and further washed with water for three times; **2f)** Pure nanosilver composite hybrid gel bead; **2g)** The hot solution of 22DAP/alginate was cooled to r.t., allowing to form interpenetrating network of hybrid gel; **2h)** An aqueous solution of $CaCl_2$ (5%, 2 mL) was then added on the top of hybrid gel to diffuse in; **2i)** A multicomponent hybrid gel bead was formed; **2j)** A 55 mmol $AgNO_3$ solution (6 mL) was added on the top of hybrid gel bead and left for 3 days then $AgNO_3$ solution was discarded carefully with the help of pipette and further washed with water for three times; **2k)** Nanosilver composite multicomponent hybrid gel.

Alginic acid is an interesting polymer gel, which is versatile, biocompatible and biodegradable.[67] Moreover sodium alginate is water soluble and forms hydrogels when mixed with Ca^{2+} ions. Gel beads by alginate can be made by drop-wise addition of alginate solution into calcium chloride solution.[68] More complex core-shell alginate beads can also be made by using another component that fills the interior of the alginate bead.[69] Smith and co-workers were the first to report the incorporation of LMWG within alginate microgel bead.[70]

Recently, we synthesized a variety of simple low molecular mass gelators staring from 2,6-diaminopyridine (DAP) for drug incorporation and release study.[46] To explore the potential of these analogues in the field of biosciences, herein, we report the *in situ* formation of silver nanocomposite **22DAP** gel and two component hybrid gel (**22DAP**/alginate system) in which alginate network provides a spherical core to compel LMWG self-assembly as shown in **Figure 3.1**. To obtain spatial control, we have

mixed the alginate polymer gel (PG) with a **22DAP** gelator. Spatially, two networks can be organised as;1) vial-filling gels with extended networks and; 2) micro-spherical gel beads. Here we have chosen to load AgNPs into **22DAP** organogel and hybrid gel beads because of their strong antibacterial and anti-biofilm properties.[5] These nanoparticles were found to be a promising antibacterial agents against several antibiotic drug-resistant bacterial strains.[34] Different polymers have also been used for the coating of AgNPs, which provides stability and also reduces the toxicity of NPs to the microbial host.[71,37] We report herewith the preparation of silver nanoparticles loaded gel beads that may be able to aid bone regeneration by inhibiting infections and be easier to handle and administer to patients because of their bead shape. A comparative AgNPs uptake and release study was also performed in single component **22DAP** gel, two component **22DAP**/alginate gel and multi-component hybrid gel beads.

3.2 Results and Discussion

The low molecular weight fatty acid amide gelator **22DAP** was synthesized by our earlier reported method[46] to form organogel (DMSO) at minimum gelation concentration (MGC) 0.5% wt/vol by a heat-cool method, whereas sodium alginate produce hydrogel upon saturation with aqueous solution of $CaCl_2$. Both gels have different assembly networks and here we have forced a distinct spatial network of two different assemblies within the multicomponent hybrid **22DAP**/PG gel.

To reveal the networking of the gelators, spatially, two networks were controlled in different ways by different preparation method.

1) The extended interpenetrating **22DAP**/PG complex gel was synthesized by heating **22DAP** (1% wt/vol) with sodium alginate (0.8% wt/vol) in 1 mL DMSO until complete dissolution of both gelators, and then the solution was allowed to cool at room

temeprature for gelation. When the gel was formed, 2 mL of aqueous solution of $CaCl_2$ (5% wt/vol) was added to the top of the gel along the side of sample vial and allowed to stand 1h for cross-linking the two networks by diffusion of Ca^{2+} ions. The thermal stability of the hybrid gel was checked by Tube Inversion Method and it was found that the alginate decreased the gel to sol transition temperature (T_{gel}) by 3^{o}C.

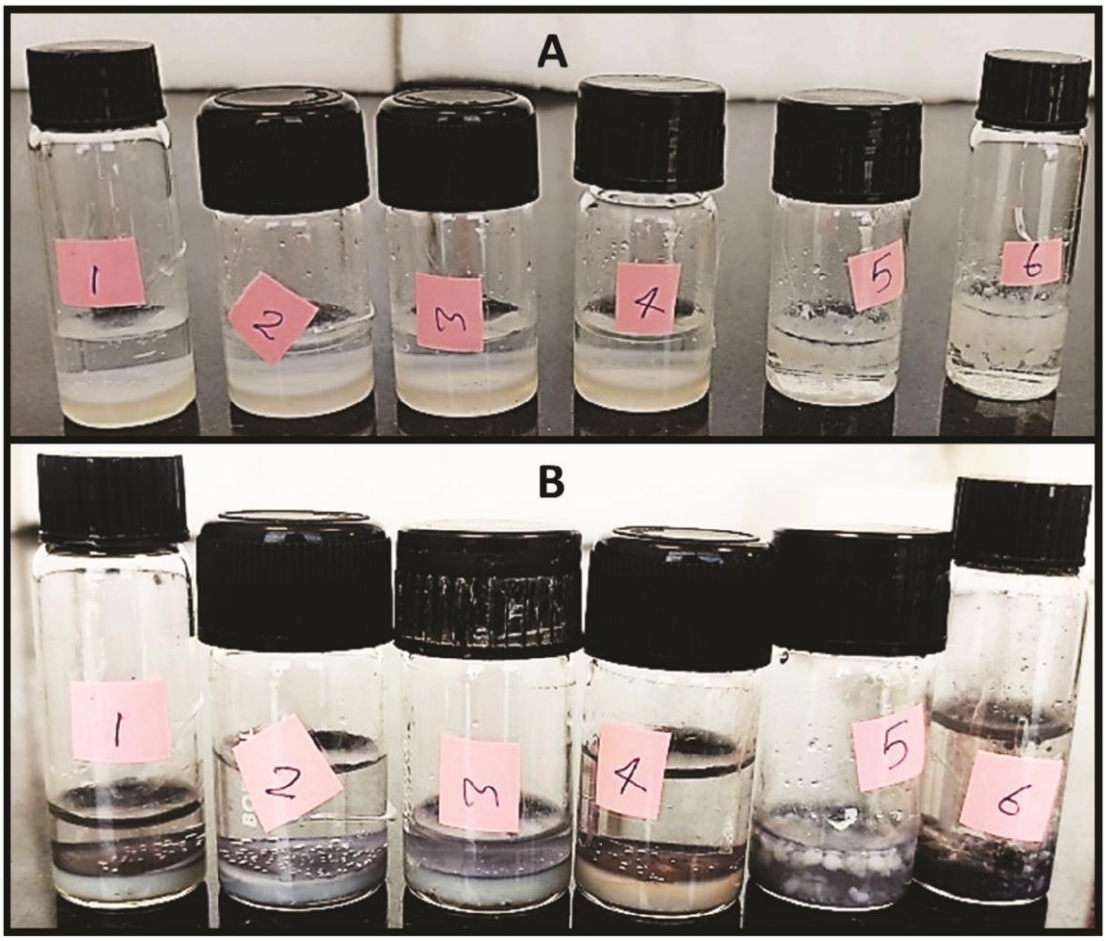

Figure 3.3. Comparison of colour change during Ag loading. Gels (from left to right): **(A): 22DAP** gel (**1** and **2**), hybrid gel extended interpenetrating networks (**3** and **4**), hybrid gel beads (**5**and**6**) before $AgNO_3$ incorporation, **(B)**: **22DAP** gel (**1**; 110 µmol of Ag and 2; 330 µmol of Ag), hybrid gel extended interpenetrating networks (**3**; 110 µmol of Ag and 4; 330 µmol of Ag), hybrid gel beads (**5**; 110 µmol of Ag and **6**; 330 µmoles of Ag) after $AgNO_3$ incorporation after 72h.

2) Gel beads with core-shell structure were prepared by mixing the same amount of **22DAP** gelator with alginate in 1 mL DMSO and the resulting solution was heated until

complete dissolution of both gelators. After that, small gel beads (ca.173.653 µm diameter) were formed by dropwise addition of the prepared hot solution (10 µL) to a $CaCl_2$ (5% wt/vol) aqueous solution, by interpenetrating the alginate with **22DAP** network on simultaneously cooling.

A single-component **22DAP** gel (in the vial) was prepared as a control material. After that, these gels were loaded with silver, where*in situ* AgNPs were formed by adding the $AgNO_3$ to the gel samples with different concentration (2 and 6 mL of a 55 mM solution) and left for 3 days to interact.

The colour of **22DAP**/PG hybrid gel was changed to brown due to diffusion of Ag^+ ions and reduction of Ag^+ ions to Ag(0) as shown in **Figure 3.3** and **3.4**. However, the colour of **22DAP** gel was not much changed due to either the presence of Ag(I) ions or less reduction of Ag(I) to Ag(0) NPs (as shown in **Figure 3.4B**). After three days, the supernatant was taken out and gels were washed with water several times. A schematic representation for the preparation of nanosilver composite single component **22DAP** gel, **22DAP**/alginate hybrid gel and hybrid gel beads is shown in **Figure 3.2**.

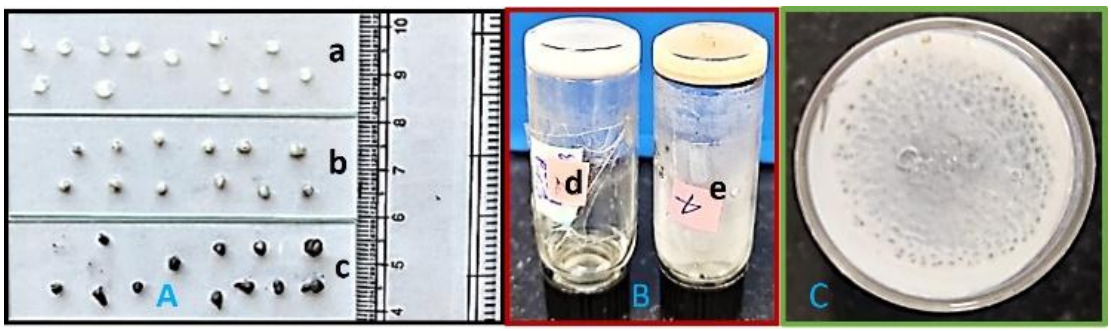

Figure 3.4. (A): Comparison of colour change between **22DAP**/alginate hybrid gel beads (**a**) before $AgNO_3$ incorporation and (**b** and **c**) after $AgNO_3$ incorporation (72h) with 110µmol and 330µmol $AgNO_3$,respectively; **(B)**: Comparison of colour change in **22DAP** gel (**d**) and **22DAP**/alginate interpenetrating hybrid gel after $AgNO_3$ incorporation (**e**); **(C)**: Photograph of inverted sample vial of **22DAP** gel after $AgNO_3$ incorporation.

The formation of nanosilver was confirmed by Transmission Electron Microscopy (TEM) images, showing that the majority of nanosilver are in the range of <10 nm in diameter for **22DAP**/PG hybrid gel beads **(Figure 3.5)** and for control experiment **22DAP** gel (**Figure 3.6**).

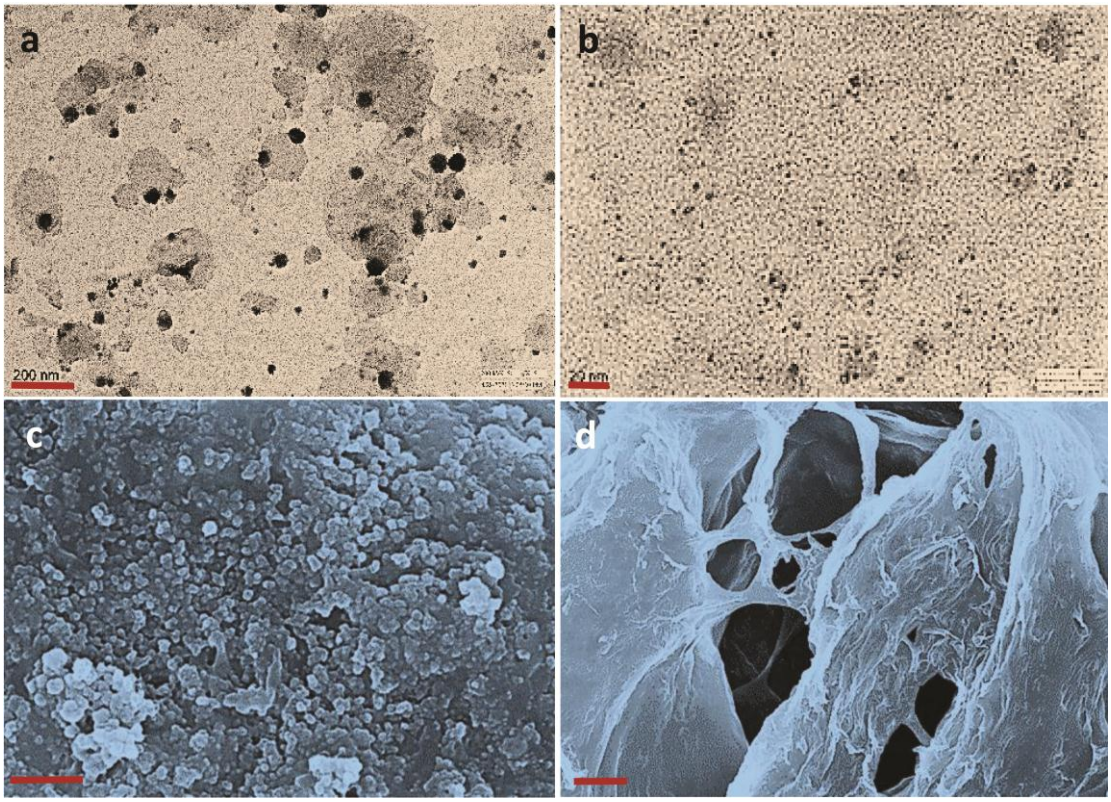

Figure 3.5. TEM images of nanosilver composite **22DAP**/alginate gel beads (scale bars from **a** to **b**: 200 and 20 nm, respectively); **c**) SEM image of **22DAP**/alginate gel bead (scale bar = 2 μM); **d**) SEM image of nanosilver composite **22DAP**/alginate hybrid gel bead (scale bar = 2 μM).

Smith and co-workers[44] reported that Ag can be incorporated in calcium alginate gels, but the Ag incorporated alginate gel had no colour indicating that either reduction of Ag^{+} ions to Ag^{0} NP is less or may be Ag is present as Ag^{+} ions and alongwith alginate gel have less control over AgNPs size with TEM (1–50 nm diameter), having irregularity and directed to forming larger particles by aggregation among a diameter >150 nm.

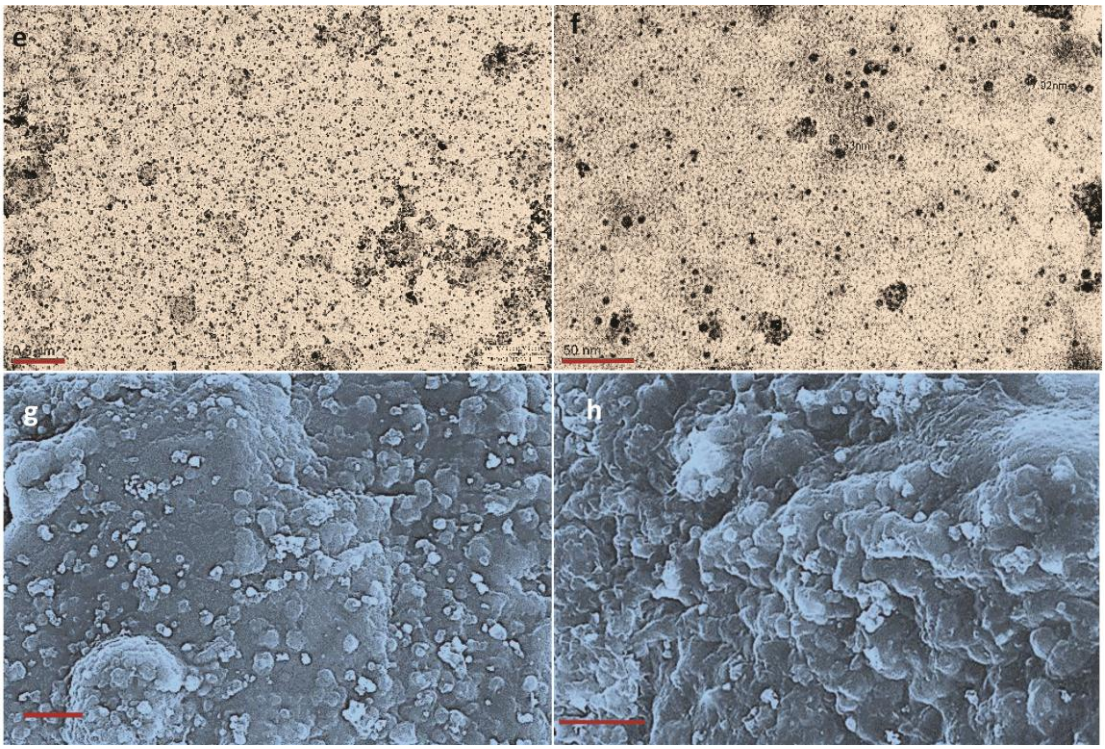

Figure 3.6. TEM images of nanosilver composite **22DAP** gel, scale bars **e** (500 nm) and **f** (50 nm); **g**) SEM images of nanosilver composite **22DAP** gel (scale bar g (10 µM) and **h** (4 µM).

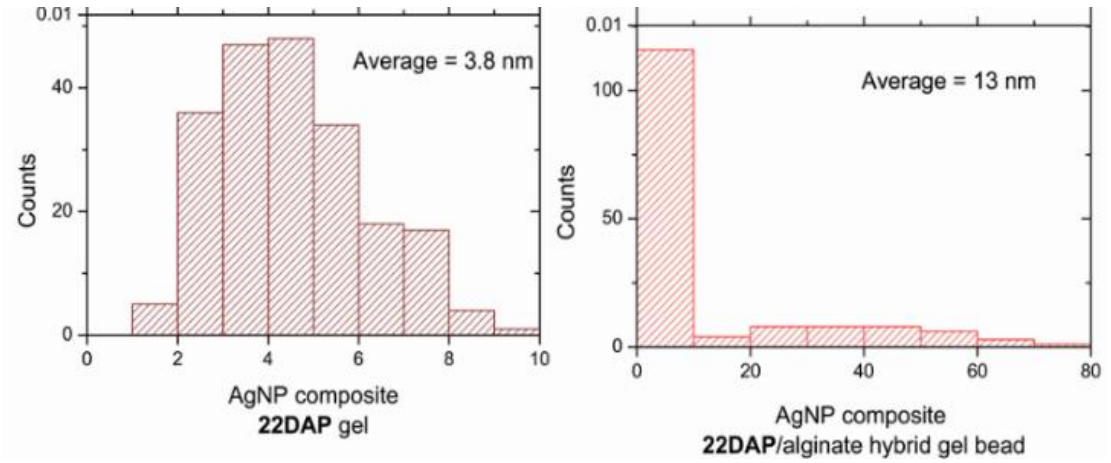

Figure 3.7. Size distribution of NPs in nanosilver composite **22DAP** gel (I) and nanosilver composite **22DAP**/alginate hybrid gel beads (II).

It has also been reported that formation of AgNPs in alginate gels is usually induced by heating, UV exposure or pH manipulation.[72] No doubt, AgNPs loaded alginate gels have become very attractive due to their anti-microbial characterstics.[73] Here, in our

system, single component **22DAP** gel and hybrid gel beads, size of AgNPs was significantly better controlled (**Figure 3.5** and **3.6**). Briefly, the incorporation of AgNPs can be better induced in the presence of **22DAP**. The quantity of Ag uptake in the gels was estimated by residual supernatant solution.

For the determination of the amount of Ag incorporation in the gels, precipitation titrations were performed using NaCl (1mM) as a titrate and K_2CrO_4 as an indicator. While the supernatant was taken as a titrant for the estimation of the remaining Ag in the supernatant solution (i.e., the Ag that was not loaded in the gel) and, by this, the quantity of incorporated Ag into the gel was calculated (**Table 3.1**).

Table 3.1. Determination of Ag(I) uptake in **22DAP** gel, **22DAP**/alginate two component hybrid gel and in multicomponent hybrid gel beads by precipitation titration technique

Gel	Loading of **22 DAP** gelator (wt/vol.)	Loading of Alginate (wt/vol.)	Ag(I) loaded on to the gel (mmol)	Ag(I) incorporated/mL in gel (mmol)	Ag(I) incorporated (%)
22DAP	1%	-	0.110	0.073	66.9
"	1%	-	0.330	0.090	27.3
22DAP/Alginate[a]	1%	0.8%	0.110	0.070	63.6
"	1%	0.8%	0.330	0.159	48.2
Gel bead[b]	1%	0.8%	0.110	0.106	96.4
"	1%	0.8%	0.330	0.210	69.7

[a]Extended interpenetrated network. [b]22DAP/alginate gel bead

It was noted that when the less concentration of $AgNO_3$ (110 µmol)was used for loading into the gels, maximum uptake was observed in case of extended hybrid **22DAP**/alginate gel beads (106 µmol of $AgmL^{-1}$ of gel) due to large surface area, while in case of **22DAP** the Ag uptake was less (73 µmol of $AgmL^{-1}$ of gel) and least incorporation of Ag was obtained in case of extended interpenetrating hybrid gel

(70 µmol of $AgmL^{-1}$ of gel) due to interaction of alginate with **22DAP** in case of interpenetrating network. Though, when the gels were exposed to higher amount of $AgNO_3$ (330 µmol of $AgNO_3$), the uptake of Ag was increased in all the cases, 90 µmol of Ag mL^{-1} of **22DAP** gel, 159 µmol of Ag mL^{-1} of interpenetrating hybrid gel and 230 µmol of Ag mL^{-1} of extended gel beads. The multi-component gel beads contain 23.1 µmol of **22DAP** mL^{-1}, and which shows that the gelator can take up approximately 9-10 equivalents of Ag, gelator in interpenetrating hybrid gel can take up 6-7 equivalents of Ag, and gelator in **22DAP** gel can take up 3-4 equivalents of Ag. However, it was reported that, calcium alginate can take up only 2-3 equivalents of Ag and also have less control over the size of AgNPs.[44]

The morphologies of gel beads, nanocomposite gel beads (**Figure 3.5; c** and **d**) and nanocomposite **22DAP** xerogel (**Figure 3.6; g** and **h**) were determined using Scanning Electron Microcopy. Xerogels of the nanocomposite gel beads and gels were prepared by deep freeze drying method. The SEM images demonstrated that gel beads and **22DAP** gel had porous morphology, which favours the formation of nanocomposites by providing pores (within the nanofibre surface) for the filling Ag(I) ions and systematically developed nanoparticles. These Ag(I) ions not only filled into the pores, but also the gap between the adjacent extended penetrating network of the hybrid gel bead nanofibres, improving intermolecular interactions[74] and hence providing thermal stability.

Table 3.2. T_{gel} values for gels formed by **22DAP** gelator and the **22DAP**/ alginate multicomponent interpenetrating gel with and without AgNPs

Gel	Solvent (1 mL)	Loading of **22 DAP** (wt/vol.)	Loading of Alginate (wt/vol.)	$AgNO_3$ loaded in gel (mmole)	T_{gel} (°C)[a]
22DAP	DMSO	1%	-	-	36
"	DMSO[b]	1%	-	-	77
"	DMSO	1%	-	0.110	75
"	DMSO	1%	-	0.330	72
22DAP/Alginate	DMSO	1%	0.8%	-	33
"	DMSO[b]	1%	0.8%	-	55
"	DMSO	1%	0.8%	0.110	80
"	DMSO	1%	0.8%	0.330	80

[a]Tube Inversion Method; [b]Saturated with 5% $CaCl_2$ solution;
T_{gel} = Gel-to-sol phase transition temperature

The thermal stability was measured as the gel-sol transition temperature (T_{gel}) using a simple Tube Inversion Method (**Table 3.2**). The T_{gel} of the **22DAP** gel (1% wt/ vol) in DMSO was 36°C, Whereas after being saturated with 2 mL aqueous $CaCl_2$ solution (5% wt/vol), the T_{gel} increased to 77°C, indicating that the diffusion of Ca^{2+} ions and H_2O molecules helps the fibre-fibre interactions. Whereas, in the presence of Ag loading (110µmol and 330 µmol of $AgNO_3$ added from the top of the gel), decreased the T_{gel} to 75°C and 72°C, respectively, showing that the loading of AgNPs disturbs the fibre-fibre interactions. Whereas, the T_{gel} value of the **22DAP** /alginate hybrid gels (1% wt/vol of **22DAP** and 0.8% wt/vol of alginate) in DMSO was 33°C, indicating that alginate decreased the fibre-fibre interaction in hybrid gel (in DMSO), but on saturating this gel with 2 mL aqueous $CaCl_2$ solution (5% wt/vol), the T_{gel} increased to 55°C, indicating that diffusion of Ca^{2+} ions and H_2O molecules helps the fibre-fibre interactions and the T_{gel} of the AgNPs loaded hybrid gel was 80°C indicating that the presence of the AgNPs increases the thermal stability of AgNPs loaded hybrid gel. It was already known that generally nanoparticle additives can stiffen the gelatinous materials.[74]

Table 3.3. Amount of Ag(I) incorporated in 1 mL gel beads used for the release study. All the samples from 1 to 9 were 1 mL **22DAP**/alginate hybrid gel beads, and in each sample 6 mL of $AgNO_3$ solution (55 mM) was added to incorporate Ag(I) and these nine samples in triplicates (**a**, **b** and **c**) were prepared for release study of Ag(I) at different time intervals.

Sample code	mmol of Ag(I) incorporated into the gel beads mL^{-1}	Ag(I) incorporated into gel beads (%)
1a	0.210	63.6
1b	0.230	69.7
1c	0.220	66.7
2a	0.220	66.7
2b	0.230	69.7
2c	0.200	60.6
3a	0.210	63.6
3b	0.180	54.5
3c	0.220	66.7
4a	0.220	66.7
4b	0.210	63.6
4c	0.230	69.7
5a	0.230	69.7
5b	0.200	60.6
5c	0.220	66.7
6a	0.200	60.6
6b	0.180	54.5
6c	0.220	66.7
7a	0.220	66.7
7b	0.210	63.6
7c	0.210	63.6
8a	0.220	66.7
8b	0.200	60.6
8c	0.230	69.7
9a	0.210	63.6
9b	0.220	66.7
9c	0.220	66.7

Release study of Ag(I) ions: The **22DAP**/alginate gel beads (10 µL volume/gel bead) were prepared and washed several times with followed by dipping the gel beads (1 mL) in 6 mL of a 55 mM solution of $AgNO_3$ for 72 h and after that the supernatant was used to determine the exact amount of loaded Ag(I) by doing precipitation titration

(explained in **Table 3.3**). For reproducibility of data, each sample was prepared in triplicates.

Calculation for amount of Ag incorporated into the gels/gel beads

Volume of NaCl used for titration = 1 mL

Molarity of NaCl used = 1 mM

Molarity equation

In case of **1a** (**Table 3.3**),

$M_1 \times V_1$ (NaCl) = $M_2 \times V_2$ (Volume of supernatant used for titration i. e. not incorporated)

1mM x 1000 µL = M_2 x 50 µL

M_2 = 20 mM

Number of moles of Ag retained in I mL supernatant = 20/1000 = 0.020 mmol

Number of moles of Ag retained in 6 mL supernatant = 0.120 mmol

Number of moles of Ag allowed for incorporation = 0.330 mmol

Number of moles of Ag incorporated with in gel beads (**1a**) = 0.330 – 0.120 = 0.210 mmol

Similarly, In case of **1b** (**Table 3.3**), for V_2 = 60 µL

After calculation,

M_2 = 16.66 mM

Number of moles of Ag retained in I mL supernatant = 16.66/1000 = 0.0166 mmol

Number of moles of Ag retained in 6 mL supernatant = 0.100 mmol

Number of moles of Ag allowed for incorporation = 0.330 mmol

Number of moles of Ag incorporated with in gel beads (**1b**) = 0.330 – 0.100 = 0.230 mmol

Ag (I) incorporated into gel beads (%)

$$= \frac{mmol\ of\ Ag\ incorporated\ obtained\ from\ titration\ [x]}{mmol\ of\ Ag\ allowed\ for\ incorporation\ into\ gels\ (0.330\ mmol)} \times 100 = 63.6\%$$ (**Table 3.3**, **1a**)

Note: All calculations have been made in the same way

Table 3.4. Ag(I) released from each sample

Sample code	Time (h)	Ag (I) released from beads ($\mu mol\ mL^{-1}$)	Release of Ag (I) (%)	Average release (%)	Standard deviation
1a	0.5	0.0066	3.14		
1b	0.5	0.0073	3.17	3.31	0.27
1c	0.5	0.0080	3.63		
2a	1.0	0.0080	3.63		
2b	1.0	0.0100	4.34	3.76	0.53
2c	1.0	0.0066	3.30		
3a	2.0	0.0080	3.80		
3b	2.0	0.0057	3.16	3.53	0.33
3c	2.0	0.0080	3.63		
4a	3.0	0.0080	3.63		
4b	3.0	0.0073	3.47	3.52	0.09
4c	3.0	0.0080	3.47		
5a	4.0	0.0080	3.47		
5b	4.0	0.0073	3.65	3.47	0.17
5c	4.0	0.0073	3.31		
6a	5.0	0.0066	3.30		
6b	5.0	0.0061	3.38	3.33	0.04
6c	5.0	0.0073	3.31		
7a	24	0.0080	3.63		
7b	24	0.0073	3.47	3.52	0.09
7c	24	0.0073	3.47		
8a	48	0.0100	4.54		
8b	48	0.0080	4.00	4.29	0.27
8c	48	0.0100	4.34		
9a	72	0.0080	3.81		
9b	72	0.0100	4.54	4.29	0.42
9c	72	0.0100	4.54		

Smith and co-workers[44] reported that hybrid gel beads incorporated with AgNPs exhibited antimicrobial properties similar to those of extended hybrid gel. By using the precipitation titration technique, we have calculated the amount of Ag(I) released from

AgNPs-loaded gels (**22DAP** gel, interpenetrating hybrid gel and the interpenetrating hybrid gel beads). The released amount of Ag(I) ions was determined by dipping the AgNPs-loaded gels and gel beads in 2 mL of H_2O, and after a particular time interval, the release quantity of Ag(I) ions was checked by titrating the supernatant solution (titrant) with 1 mM NaCl (titrate) in the presence of K_2CrO_4 indicator(5%).

For better precession, the titration was done, by slow addition of titrant (5 µL drop) to the titrate with stirring. All the results were obtained in triplicates for reproducibility (as explained in **Table 3.4**).

Calculation for amount of Ag released from the gels/gel beads (Table 3.4, 1a)

Volume of NaCl used for titration = 200 µL

Molarity of NaCl used = 1 mM

Molarity equation

In case of **1a (Table 3.4)**,

$M_1 \times V_1$ (NaCl) = $M_2 \times V_2$ (Volume of supernatant used for titration i.e. not incorporated)

1mM x 200 µL = M_2 x 60 µL

$$M_2 = 3.33 \text{ mM}$$

Number of moles of Ag released in 1 mL of water= 3.33/1000 = 0.0033 mmol

Number of moles of Ag released in 2 mL of water= 0.0066 mmol

Similarly, In case of **1b (Table 3.4)**, for V_2 = 55 µL

After calculation,

$$M_2 = 3.63 \text{ mM}$$

Number of moles of Ag released in 1 mL of water = 3.63/1000 = 0.00363 mmol

Number of moles of Ag released in 2 mL of water = 0.0073 mmol

Ag(I) released from gel beads (%)

$$= \frac{mmol\ of\ Ag\ released\ obtained\ from\ titration\ [y]}{mmol\ of\ Ag\ incorporated\ obtained\ from\ titration\ [x]} \times 100 = 3.14\%$$ (**Table 3.4**, **1a**)

Note: All calculations have been made in the same way

Comparative release study of Ag(I) from AgNPs-loaded gels

For a comparative study, using the same procedure, we also quantified the Ag(I) released from AgNPs-loaded interpenetrating hybrid gel (**Table 3.5** and **3.6**) and AgNPs-loaded **22DAP** gel (**Table 3.7** and **3.8**). For data reproducibility, all results were obtained in triplicates.

Release of Ag(I) from AgNPs-loaded gel beads: It was revealed that a small amount of Ag(I) (ca. 3.31%) was initially released from the gel beads, but even after 24h, only 3.52% of Ag(I) ions were released from the silver nanocomposite hybrid gel beads meaning that no effective silver ions were released after 30 minutes. After 48 h, the release amount of Ag(I) was 4.29% (**Figure 3.8**). After 72 h, the supernatant medium was replaced with fresh water, and it was observed that only 0.2% silver ions were released. This would propose that any prolonged antibacterial activity associated with the gel beads is more likely to be associated with slower AgNPs release.

Release of Ag(I) from interpenetrating extended 22DAP/alginate gel: It was observed that in case of extended gel, there was slow release of Ag(I) ions from the AgNPs-loaded extended gel, and after 24 h, 7.23% release of Ag(I) was obtained and after that no effective release was obtained as shown in **Figure 3.8**.

Release of Ag(I) from AgNPs-loaded 22DAP gel: In case of AgNPs-loaded **22DAP** gel, release amount of Ag(I) was higher than that of both the gel beads and

interpenetrating extended gel, and 9.01% release amount of Ag(I) was obtained after 72 h. The comparative release study of Ag(I) from silver nanocomposite gels and gel beads is shown in **Figure 3.8.**

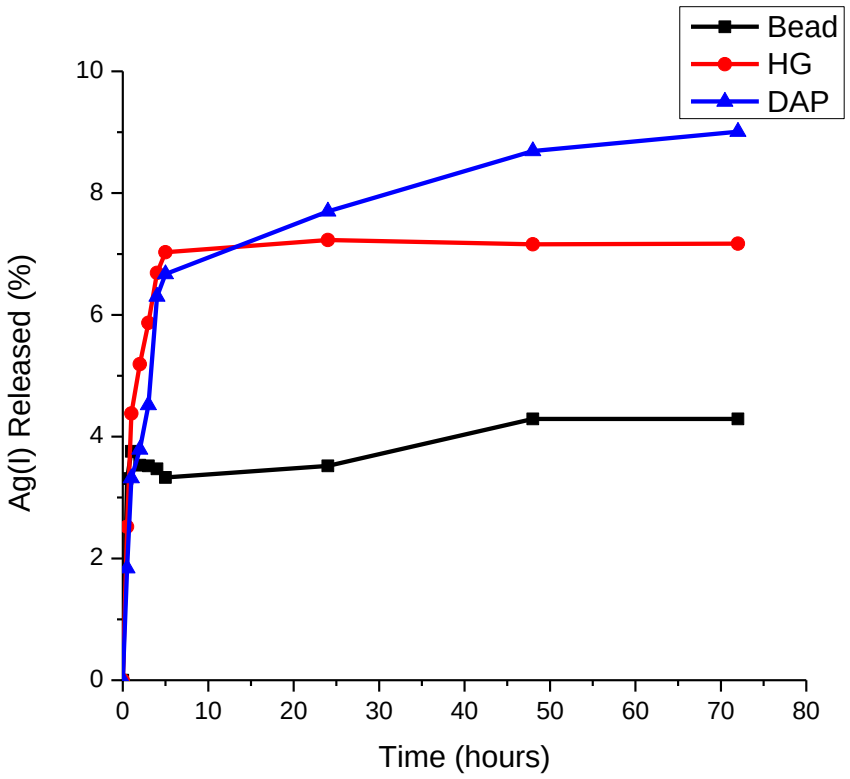

Figure 3.8. Release amount of Ag(I) ions from the **22DAP** (blue line), **22DAP**/alginate extended gel (red line) and 22DAP/alginate gel beads (black line) with time.

3.3 Fourier transmission infrared spectroscopy (FT-IR) analysis

For FTIR analysis, the gel samples were dried by lyophilisation and spectra were recorded in the range 667-4000 cm^{-1}, by taking a small amount of xerogel powder. The FT-IR spectra of bead (**a**); loaded bead (**b**); sodium alginate (**c**), $AgNO_3$ (**d**), **22DAP(e)**, loaded gel (**22DAP**) **(f)**, are given in **Figure 3.9**. In the spectrum of native **22DAP** (**e**), there are characteristic peaks at 3288 and 3164 cm^{-1}, which are attributed to NH bond stretching of NH_2. The peaks at 2918 and 2850 cm^{-1} corresponds to CH stretching of alkyl chains whereas peaks at 1673 cm^{-1} corresponds to the stretching vibration of

amide carbonyl >C=O and other characteristic peaks of **22DAP** are 2375, 2313, 1659, 1611, 1532, 1466, 1357, 1297, 1254, 1170, 1025, 802 and 710 cm^{-1}. In the spectrum of $AgNO_3$**(d),** the characteristic peaks are 3567, 1870, 1840, 1750, 1641, 1532, 1472, 1297, 844 and 784 cm^{-1}. In case of loaded gel 22DAP **(b),** the IR peaks are 2957, 2915, 2843, 1659, 1629, 1557, 1460, 1321, 1254, 1158, 1091, 1019, 953, 862, 796 and 711 cm^{-1}. In this spectra the peaks 2915, 2843, 1659, 1460, 1254, 1158 and 710 cm^{-1} are relative peaks of **22DAP**, while the peaks 1629, 1557, 862 and 796 cm^{-1} are relative to the characteristic peaks of AgNPs. Sodium alginate **(c)**, consist a strong peak at 3435 cm^{-1} which corresponds to the O-H stretching vibration frequency while other characteristic peaks are at 2926, 2854, 2370, 2298, 1750, 1617, 1514, 1420, 1309, 1201, 1097 and 1030 cm^{-1} (**c**).

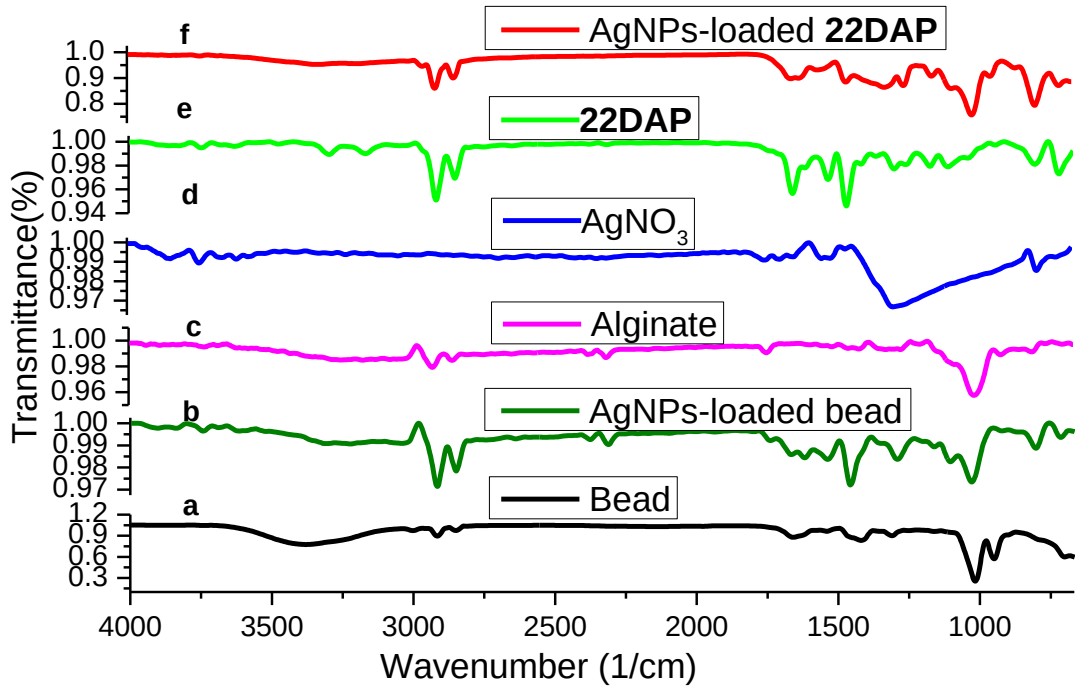

Figure 3.9. IR spectra of xerogels of **22DAP**/alginate bead (a), AgNPS-loaded 22DAP/ alginate bead (b), sodium alginate (c), $AgNO_3$ (d), **22DAP** (e), and AgNPs-loaded **22DAP** xerogel (f).

FT-IR spectra of bead xerogel (**a**) had band at 3422, 3367, 2912, 2850, 1651, 1466, 1324 and 1014 cm^{-1} respectively relative to the O-H stretching vibration frequency of alginate and the peaks at 2912 and 2850 cm^{-1} corresponds to CH stretching of alkyl chains whereas peaks at 1651 cm^{-1} corresponds to the stretching vibration of amide carbonyl >C=O of native xerogel **22DAP**, respectively. The FT-IR spectra AgNPs composite bead (**b**) had band at 3560, 3428, 3363, 3045, 2917, 2839, 2386, 2295, 1747, 1655, 1616, 1535, 1452, 1348, 1272, 1211, 1158, 1090, 1013, 870, 805 and 792 cm^{-1}. The peaks 3428, 3363, 2917, 2839, 1655, 1452 and 1013 cm^{-1} are corresponding to the characteristic peaks of xerogel bead while the peaks at 3560, 1747, 1616, 1535, 1272 and 792 cm^{-1} are corresponding to peaks of AgNPs.

3.4 Conclusion

We have reported a mild and efficient process for the preparation of single component silver nanocomposite **22DAP** gel, expanded two component **22DAP**/alginate hybrid gel and multicomponent **22DAP**/alginate hybrid gel beads for antimicrobial applications. Silver nanoparticle uptake was studied in these systems, where there was an *in situ* reduction of Ag(I) to Ag(0). Furthermore it was observed that the alginate polymer gel enables the gelator to control the shape and forms the core-shell structured beads. In case of **22DAP** gel, the AgNPs disturbs the interactions and slightly reduce the thermal stability of gel. In contrast, in the case of the hybrid gel, the thermal stability of the expanded hybrid gel was enhanced by AgNPs. Briefly, the polymer gel enables the **22DAP**/alginate gel to shape the gelator into a core-shell gel bead, which will be easy to use and operate. Furthermore the polymer gel increases the Ag(I) uptake in case of

hybrid gel beads and decreases both the release rate and extent of Ag(I) ions from AgNPs-loaded hybrid gel beads. It was observed that the uptake of Ag(I) ions was ~4 equivalents in the case of **22DAP**gel, whereas it was increased to ~10 equivalents in the case of hybrid gel beads. Whereas, calcium alginate can take up only 2-3 equivalents of Ag and has even less control over the size of AgNPs. It was also observed that both **22DAP** gel and **22DAP**/alginate gel beads have good control over the size of the AgNPs. Simultaneously, a very slow and control release of Ag(I) from AgNPs-loaded hybrid gel beads was determined, showing that only 4.29% Ag(I) was released in 72h, and then there was very little amount of Ag(I) released, which would suggest that any prolonged antibacterial activity associated with gel beads is more likely to be associated with slower AgNPs release and it is already well known that AgNPs exhibit promising antimicrobial activities. These results may provide better opportunities in the fields of biomedicine, optoelectronics and imaging investigations.

3.5 Experimental

3.5.1 Materials

2,6-Diaminopyridine, oxalyl chloride, triethyl amine and behenic acid were bought from Central Drug House and used as such. The sodium alginate and K_2CrO_4 were purchased from Sigma Aldrich. $AgNO_3$ was bought from Fischer Scientific. All solvents were distilled prior to use.

3.5.2 Methods

Nuclear Magnetic Resonance (NMR) spectra (^1H) and (^{13}C) were recorded on Bruker 400 MHz and 101 MHz spectrometer, respectively. The samples were made in

chloroform-d using tetramethylsilane (TMS) as the internal standard and chemical shift values were measured in ppm on a scale downfield from TMS and the coupling constant *J* are in Hz. The molecular mass of synthesized compound was obtained by high resolution LC-MS (Agilent) instrument. The IR spectra were obtained with FT-IR Bruker Instrument.

3.5.3 Synthesis of *N*-(6-aminopyridin-2-yl)docosanamide(22DAP) fatty acid amide gelator

22DAP fatty acid amide gelator was synthesized by our reported method (Chapter II).[24]

3.6 Gel preparation

22DAP gels

22DAP gelator (1% wt/vol) was suspended in DMSO (1 mL). The suspension was heated up to complete dissolution of the LMWG. The solution was left undisturbed to cool at room temperature, allowing formation of gel in a few minutes. The flow of gel against gravitational force was checked by inversion of the sample vial (**Figure 3.2**).

22DAP/alginate two-component hybrid gels (prolonged interpenetrating networks)

22DAP gelator (1% wt/vol in 1 mL total volume) and sodium alginate (0.8% wt/vol) was taken in 1 mL DMSO and heated up to complete dissolution of **22DAP** and alginate. The solution was allowed to stand for 1 hr to form the **22DAP**-alginate interpenetrating network. A 5.0% wt/vol $CaCl_2$ solution was then added from top of every gel to crosslink the alginate chains for 30 min. The excess

solution of $CaCl_2$ was then taken out and the gels were washed multiple times with water (**Figure 3.2**).

22DAP/alginate two-component gel beads

22DAP (1% wt/vol in 1 mL final volume) and alginate (0.8% wt/vol) were taken in 1 mL DMSO and heated until complete dissolution of **22DAP** and alginate. Then the hot solution was added dropwise (10 µL/drop) to a 5.0% wt/vol $CaCl_2$ solution. The acquired beads were filtered and washed multiple times with water (**Figure 3.2**).

3.7 AgNPs formation into gels (*in situ*)

All of these gels were washed multiple times thoroughly with water and immersed in 2 or 6 mL of $AgNO_3$ solution (55 mM) for 3 days. After 3 days, the supernatant was softly taken out with a pipette and the gels were washed multiple times by water. Here a clear colour change was noticed due to reduction of Ag(I) to Ag(0) (**Figure 3.2**).

3.8 Thermal stability

Gel-to-sol phase transition temperature (T_{gel}) was determined by a tube inversion method. The gels (in glass sample vials) were suspended in a temperature controlled oil bath with a starting temperature of 20^{o}C. The temperature of hot plate was increased by 1^{o}C per minute. After every minute flow of gels were examined by inversion tube method. The temperature was esteemed as T_{gel} at which the gels break down or started to flow along the sides of vials on inverting the sample vials.

3.9 Scanning electronic microscopy (SEM)

The nanocomposite gel, multicomponent hybrid gel beads and nanocomposite hybrid gel beads were deep freeze dried under lyophilisation and their morphology analysis was carried out with the SEM EVO18 Zeiss model.

3.10 Transmission electronic microscopy (TEM)

The TEM (Transmission Electron Microscopy) images were taken by using FEI Tecnai S Twin microscope with 200 kV operating voltage.

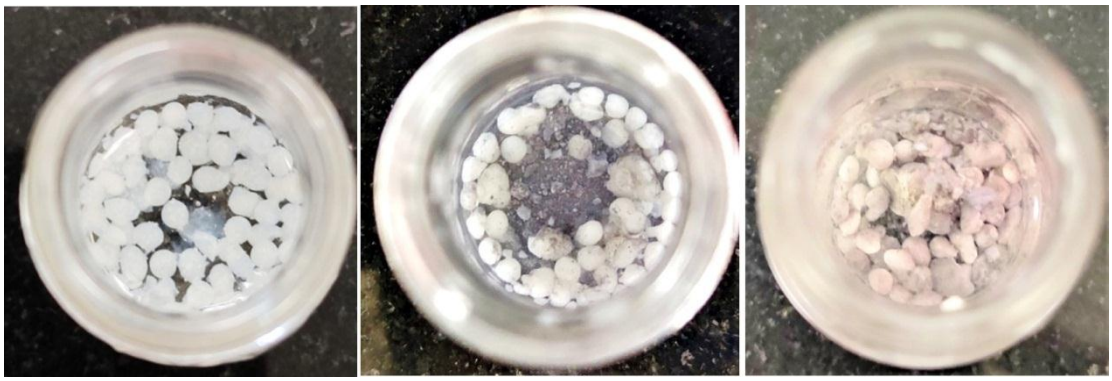

Figure 3.10. Photograph of **22DAP**/alginate gel beads from the top of the sample vials showing clear colour change during Ag(I) uptake - (***a***) without $AgNO_3$ addition, (***b***) after $AgNO_3$ (2 mL of 55 mM $AgNO_3$ solution) addition after 24 h, and (***c***) after $AgNO_3$ (6 mL of 55 mM $AgNO_3$ solution) addition after 72 h.

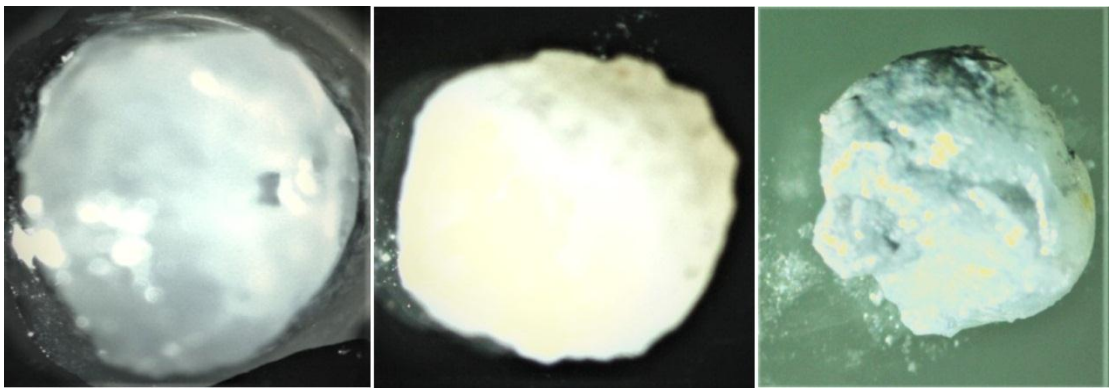

Figure 3.11. Microscopic images of **22DAP**/alginate gel beads- (***a***) gel bead before $AgNO_3$ addition, (***b***) after $AgNO_3$ (110 µmol of Ag)addition, and (***c***) after $AgNO_3$ (330 µmol of Ag) addition.

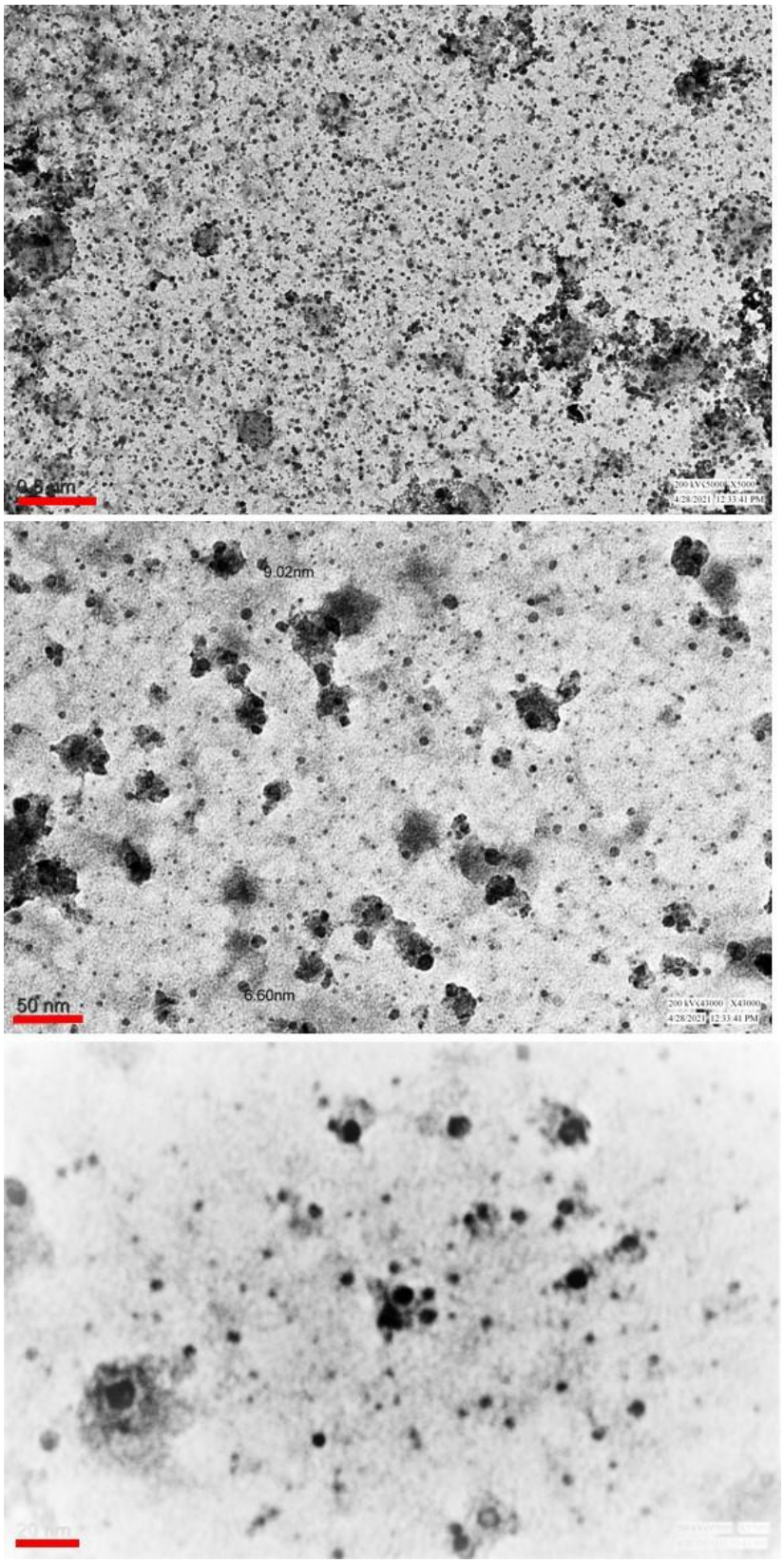

Figure 3.12. TEM images of AgNPs-loaded **22DAP** gel (scale bars from top to bottom: 500 nm, 50 nm and 20 nm, respectively).

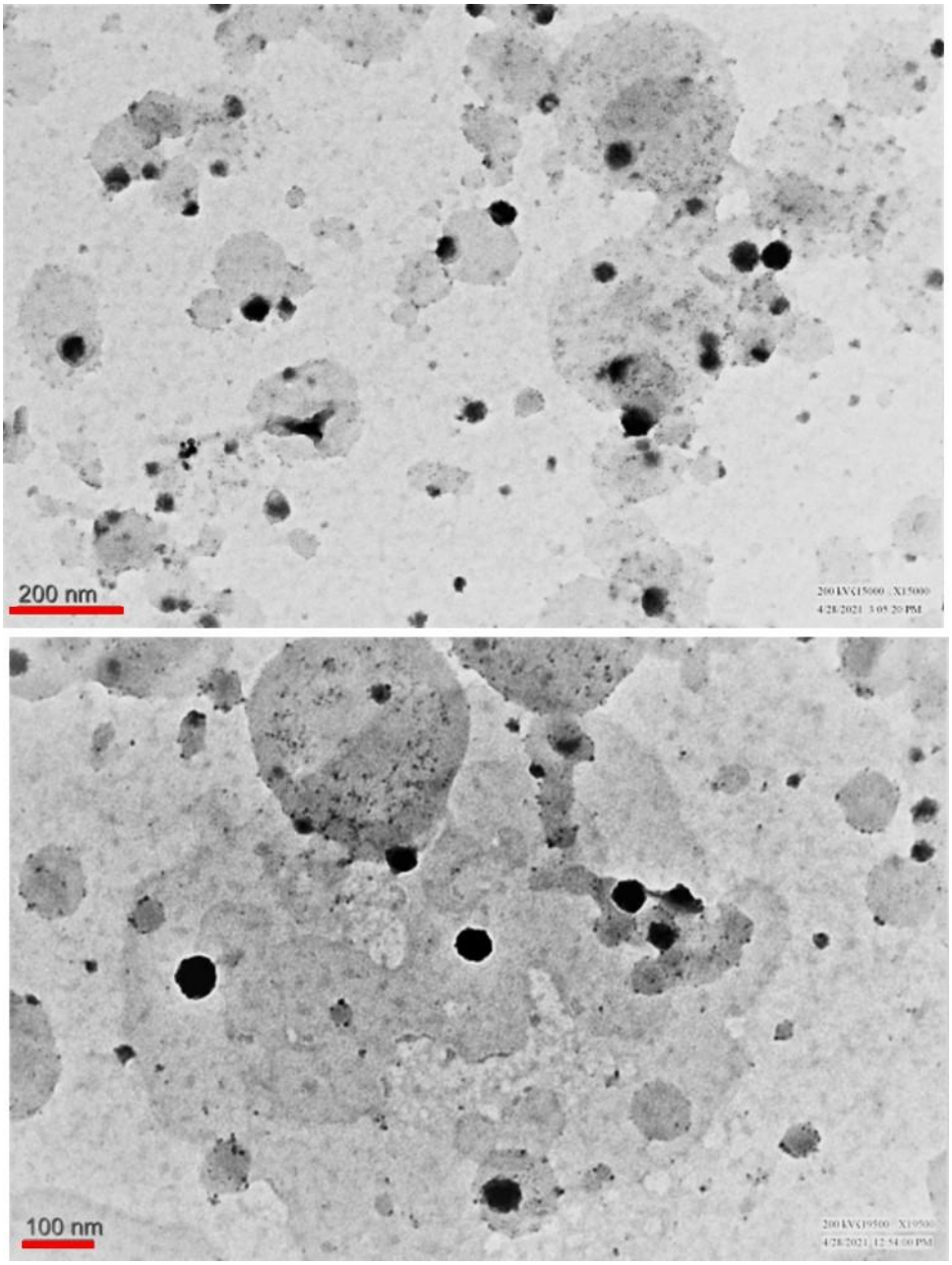

Figure 3.13. TEM images of AgNPs-loaded **22DAP**/alginate gel beads (scale bars from top to bottom: 200 nm and 100 nm, respectively).

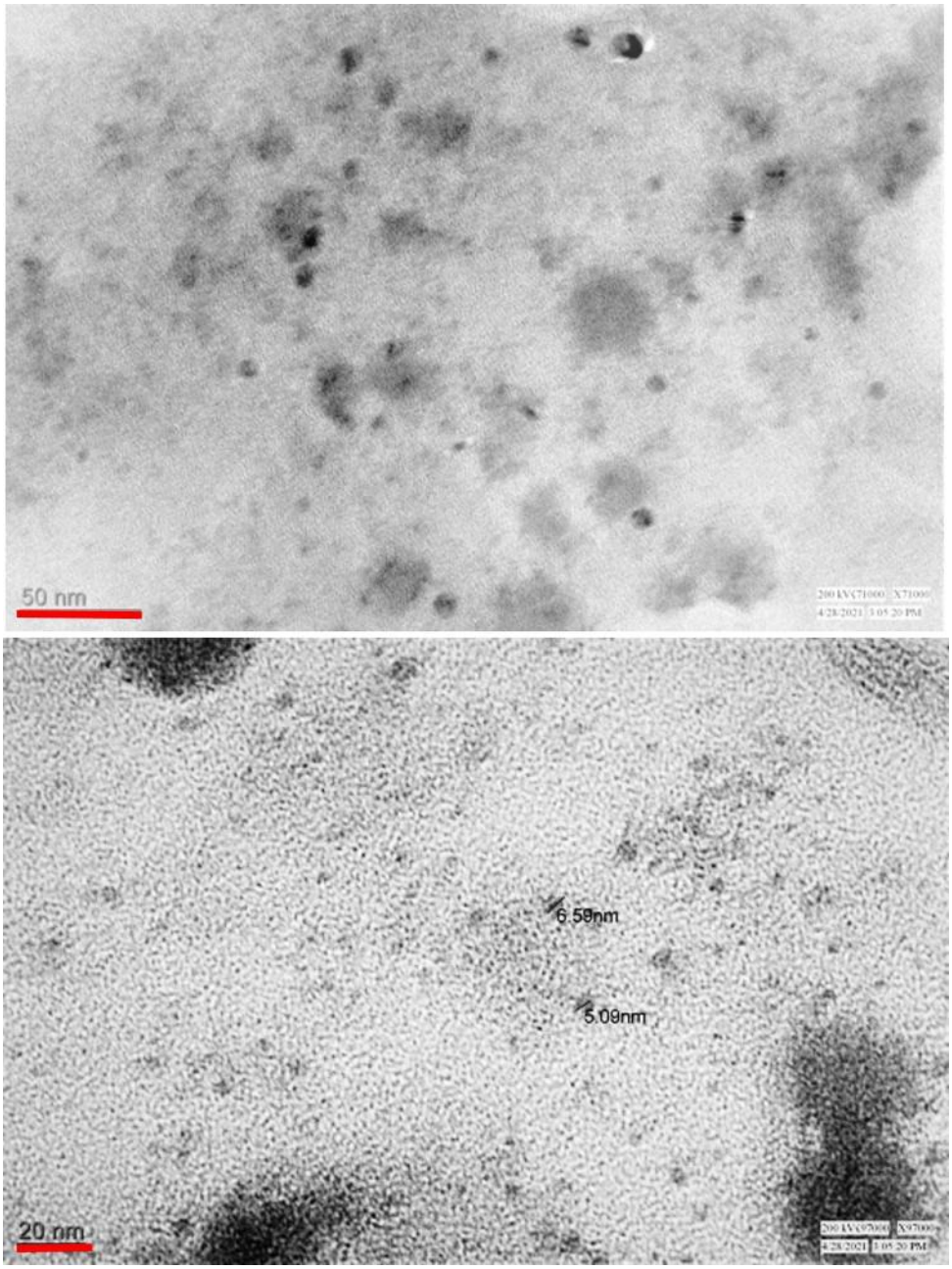

Figure 3.14. TEM images of AgNPs-loaded **22DAP**/alginate gel beads (scale bars from top to bottom: 50 nm and 20 nm, respectively).

Figure 3.15. Photograph of AgNPs-loaded **22DAP**/alginate gel beads after lyophilisation.

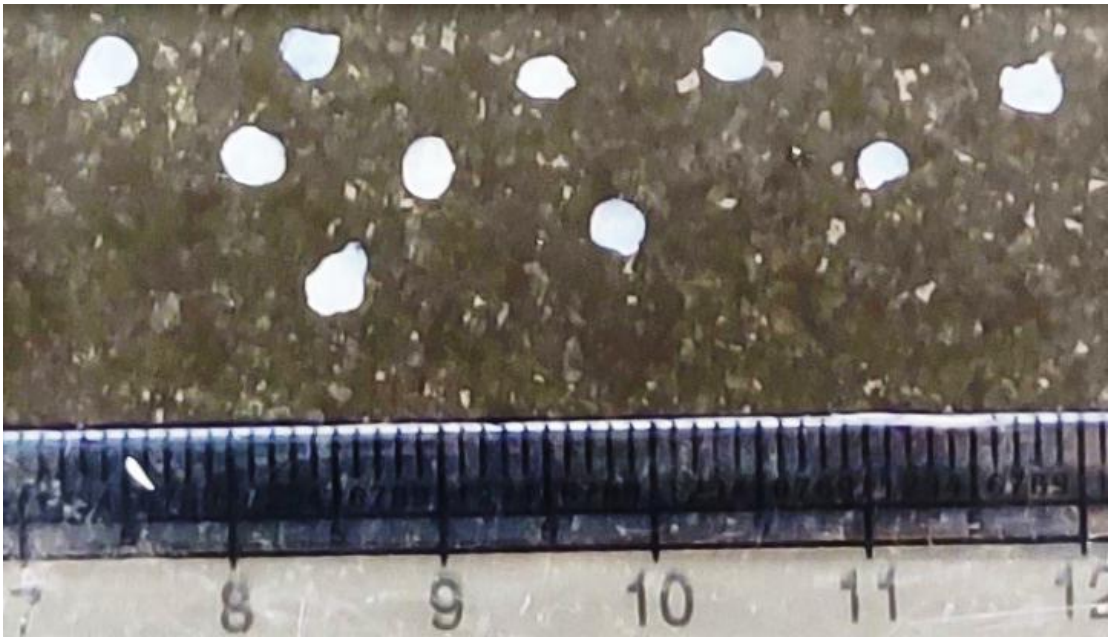

Figure 3.16. Photograph of **22DAP**/alginate gel beads on centimetre scale bar.

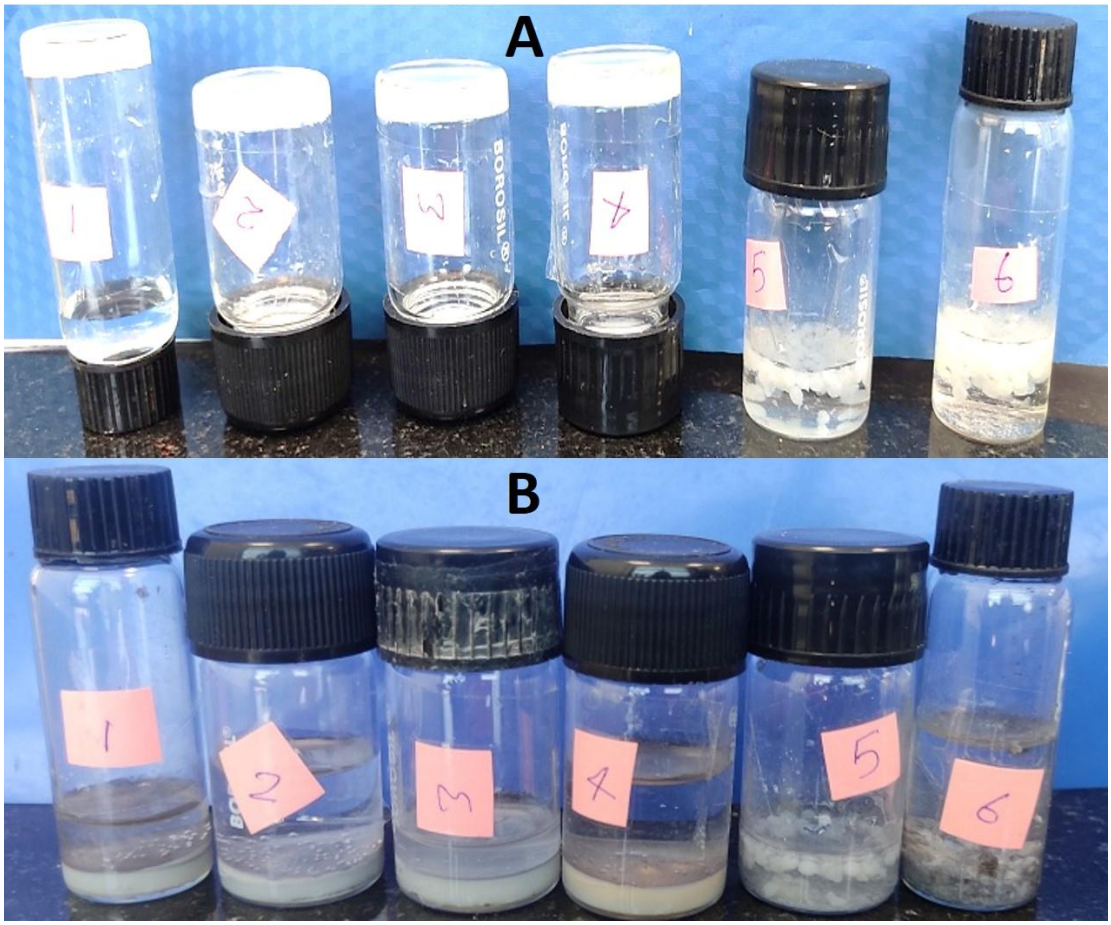

Figure 3.17. Comparison study for colour change during Ag loading. Gels (from left to right): **(A):22DAP** gel (**1**,**2**); hybrid gel extended interpenetrating networks (**3**,**4**); hybrid gel beads (**5**, **6**) before $AgNO_3$ incorporation; **(B)**: **22DAP** gel (**1**; 110 µmol of Ag and **2**; 330 µmol of Ag); hybrid gel extended interpenetrating networks (**3**; 110 µmol of Ag and **4**; 330 µmol of Ag); hybrid gel beads (**5**; 110 µmol of Ag and **6**; 330 µmol of Ag) after $AgNO_3$ incorporation after 72 h.

Table 3.5. Amount of Ag(I) incorporated in 1mL interpenetrating hybrid gel used for the release study.

Sample code	mmol of Ag(I) incorporated into hybrid gel mL^{-1}	Ag(I) incorporated into hybrid gel (%)
1a	0.159	48.2
1b	0.130	39.4
1c	0.130	39.4
2a	0.159	48.2
2b	0.159	48.2
2c	0.130	39.4
3a	0.180	54.5
3b	0.130	39.4
3c	0.159	48.2
4a	0.130	39.4
4b	0.159	48.2
4c	0.159	48.2
5a	0.130	39.4
5b	0.130	39.4
5c	0.159	48.2
6a	0.159	48.2
6b	0.130	39.4
6c	0.130	39.4
7a	0.159	48.2
7b	0.130	39.4
7c	0.159	48.2
8a	0.159	48.2
8b	0.130	39.4
8c	0.159	48.2
9a	0.159	48.2
9b	0.159	48.2
9c	0.130	39.4

Table 3.6. Amount of Ag(I) released from each AgNPs loaded interpenetrating hybrid gel sample.

Sample code	Time (h)	Ag(I) release from hybrid gel (mmol/mL)	Release of Ag (I) (%)	Average release (%)	Standard deviation
1a	0.5	0.0040	2.51		
1b	0.5	0.0033	2.53	2.52	0.01
1c	0.5	0.0033	2.53		
2a	1.0	0.0063	3.96		
2b	1.0	0.0069	4.34	4.38	0.45
2c	1.0	0.0063	4.85		
3a	2.0	0.0074	4.11		
3b	2.0	0.0082	6.31	5.19	1.10
3c	2.0	0.0082	5.16		
4a	3.0	0.0090	6.92		
4b	3.0	0.0080	5.03	5.87	0.96
4c	3.0	0.0090	5.66		
5a	4.0	0.0088	6.77		
5b	4.0	0.0101	7.77	6.69	1.12
5c	4.0	0.0088	5.53		
6a	5.0	0.0098	6.16		
6b	5.0	0.0098	7.53	7.03	0.79
6c	5.0	0.0098	7.53		
7a	24	0.0096	6.04		
7b	24	0.0112	8.62	7.23	1.30
7c	24	0.0112	7.04		
8a	48	0.0110	6.92		
8b	48	0.0110	8.46	7.16	1.17
8c	48	0.0098	6.16		
9a	72	0.0110	6.92		
9b	72	0.0112	7.04	7.17	0.33
9c	72	0.0098	7.54		

Table 3.7. Amount of Ag(I) incorporated in 1ml **22DAP** gel used for the release study.

Sample code	mmol of Ag(I) incorporated into gel (**22DAP**) mL^{-1}	Ag(I) incorporated into **22DAP** gel (%)
1a	0.090	27.3
1b	0. 108	32.7
1c	0.108	32.7
2a	0.108	32.7
2b	0.130	39.4
2c	0.090	27.3
3a	0.090	27.3
3b	0.090	27.3
3c	0.108	32.7
4a	0.090	27.3
4b	0.108	32.7
4c	0.090	27.3
5a	0.108	32.7
5b	0.090	27.3
5c	0.090	27.3
6a	0.090	27.3
6b	0.108	32.7
6c	0.090	27.3
7a	0.108	32.7
7b	0.090	27.3
7c	0.090	27.3
8a	0.130	39.4
8b	0.090	27.3
8c	0.090	27.3
9a	0.108	32.7
9b	0.108	32.7
9c	0.090	27.3

Table 3.8. Amount of Ag(I) released from each AgNPs loaded **22DAP** gel sample.

Sample code	Time (h)	Ag (I) released from gel (mmol/mL)	Ag (I) released (%)	Average (%)	Standard deviation
1a	0.5	0.0018	2.00		
1b	0.5	0.0020	1.85	1.84	0.16
1c	0.5	0.0018	1.67		
2a	1.0	0.0030	2.78		
2b	1.0	0.0050	3.84	3.32	0.53
2c	1.0	0.0030	3.33		
3a	2.0	0.0037	4.11		
3b	2.0	0.0037	4.11	3.79	0.55
3c	2.0	0.0034	3.15		
4a	3.0	0.0045	5.00		
4b	3.0	0.0042	3.89	4.52	0.57
4c	3.0	0.0042	4.67		
5a	4.0	0.0060	5.56		
5b	4.0	0.0060	6.67	6.30	0.64
5c	4.0	0.0060	6.67		
6a	5.0	0.0073	6.76		
6b	5.0	0.0065	6.02	6.67	0.60
6c	5.0	0.0065	7.22		
7a	24	0.0081	7.50		
7b	24	0.0073	8.11	7.70	0.35
7c	24	0.0081	7.50		
8a	48	0.0092	7.08		
8b	48	0.0079	8.78	8.69	1.57
8c	48	0.0092	10.22		
9a	72	0.0092	8.51		
9b	72	0.0092	8.51	9.01	0.86
9c	72	0.0090	10.00		

3.11 Rheological studies

The rheological studies of the organogel (**22DAP**) and hybrid gel are shown in the **Figure 3.18** and **3.19**. The rheological profile showed that the apparent viscosity of the HG gel is higher as compare to **22DAP** organogelgel showing better mechanical strength of HG gel as compare to organogel. From the graph, it was obtained that the shear viscosity of the oleogels was decreased on increasing the shear rate from 12 to $95s^{-1}$.

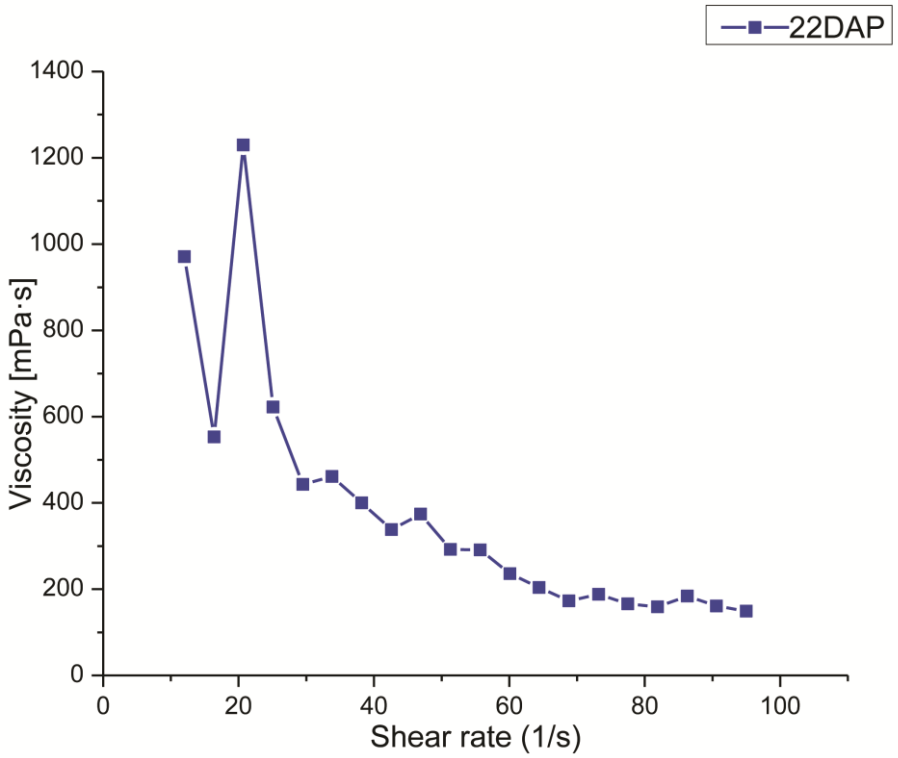

Figure 3.18. Viscosity profile of the **22DAP** organogel (DMSO) with respect to shear rate.

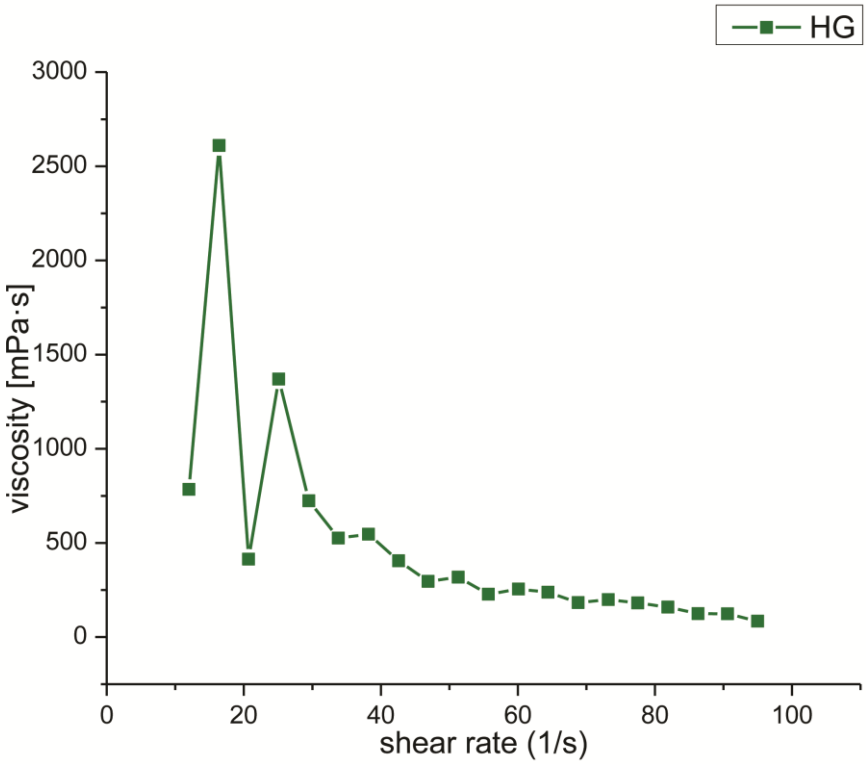

Figure 3.19. Viscosity profile of the HG with respect to shear rate.

The decrease in the shear viscosity with increase in shear rate showed the shear thinning behaviour of the gels.[75] Both the **22DAP** organogel (DMSO) and HG indicated the shear thinning behavior which is common in ointments, creams and gels.[76] The flowing nature of the **22DAP** gel and **HG** were determined by the modified power law (equation 1).[77]

$$\eta = K\,\gamma^{n-1} \quad (1)$$

Where η is the apparent viscosity (Pa.s), K is the flow consistency index, γ is shear rate (s−1) and n value determines the flowing behavior of the gels. From **equation 1**, it was calculated that the n values of the gels were < 1 which presented that the gels follows the non-Newtonian pseudoplastic fluid behaviour. Pseudoplasticity is known to be important property for topical formulations, because on increasing the shear stress, the gels will penetrate good through the skin.[78,79] The semi-solid nature of **22DAP** organogel and HG provide them long term stability during storage.[78,80]

3.12 Characterization of AgNPs by EDX spectrum

Field emission–transmission electron microscopy (FE–TEM) images revealed that most of the synthesized AgNPs are spherical in shape with a diameter of < 10nm. Similar shape and size of synthesized AgNPs are reported by the previous studies.[81] The purity and composition of synthesized AgNPs are analysed using an EDX spectrometer. The EDX spectrum showed elemental signals of Ag atoms in silver nanocomposites at around 3 keV and showed uniform distribution of AgNPs in Ag nanocomposites (**Figure 3.20**). Additionally, prior studies have shown that AgNPs exhibit a sharp absorption peak nearly at 3 keV in their EDX patterns.[82]

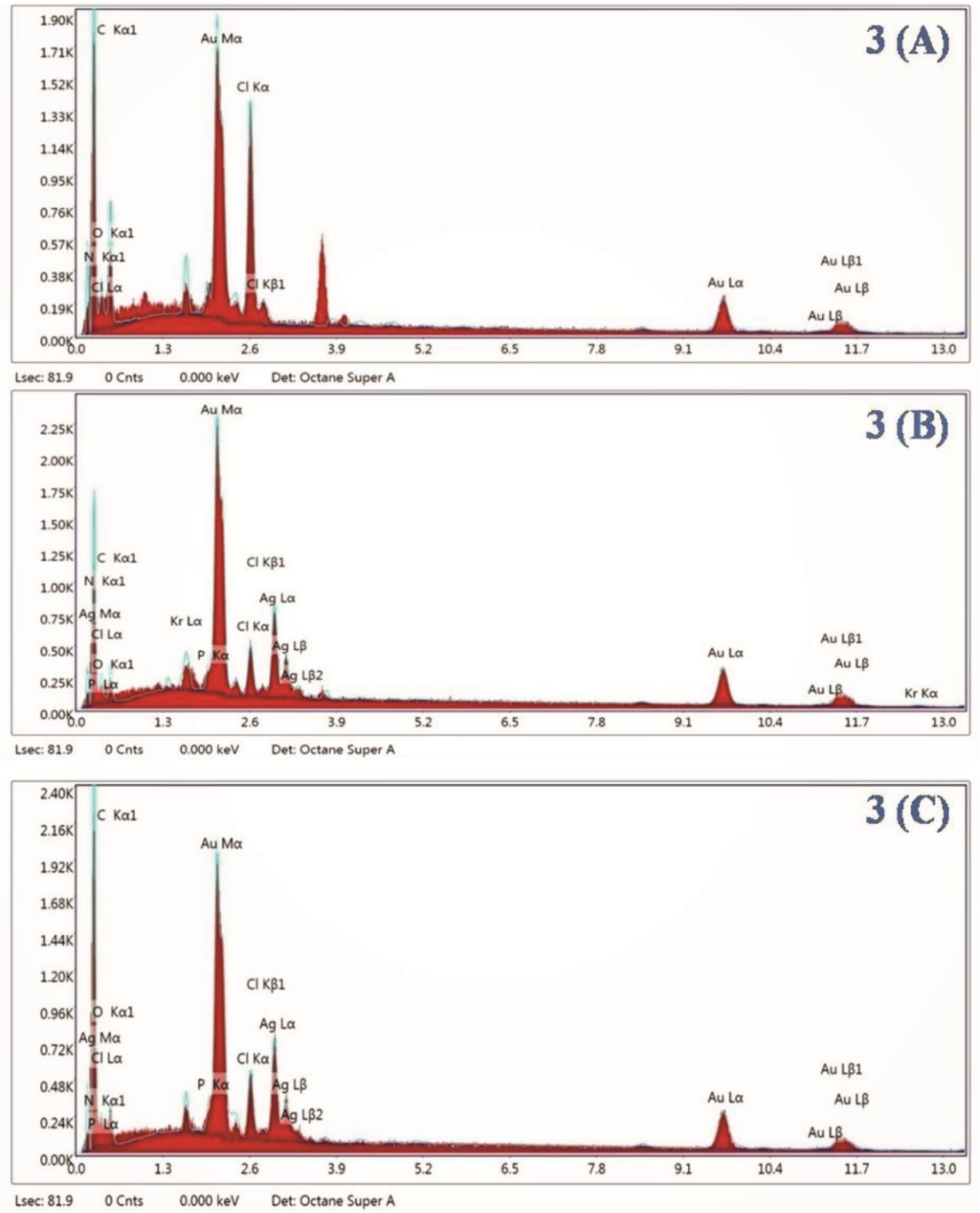

Figure 3.20. Energy dispersive X-ray (EDX) spectrum of HG beads (A), **22DAP** silver nanocomposites (B) and HG bead silver nanocomposites (C).

3.13 References

1. V. M. D'Costa, C. E. King, L. Kalan, M. Morar, W. W. Sung, C. Schwarz, D. Froese, G. Zazula, F. Calmels, R. Debruyne, *Nature*, 2011, **477**, 457–461.
2. C. A. Dos Santos, M. M. Seckler, A. P. Ingle, I. Gupta, S. Galdiero, M. Galdiero, A. Gade, M. Rai, *J. Pharm. Sci.*, 2014, **103**, 1931–1944.
3. H. Seppala, T. Klaukka, J. Vuopio-Varkila, A. Muotiala, H. Helenius, K. Lager, P. Huovinen, *N. Engl. J. Med.*, 1997, **337**, 441–446.
4. D. I. Andersson, D. Hughes, *Nat. Rev. Microbiol.*, 2010, **8**, 260–271.
5. G. Franci, A. Falanga, S. Galdiero, L. Palomba, M. Rai, G. Morelli, M. Galdiero, *Molecules*, 2015, **20**, 8856-8874.
6. N. Cassir, J. M. Rolain, P. Brouqui, *Front. Microbiol.*, 2014, **5**, 551.
7. X. Chen, H. J. Schluesener, *Toxicol. Lett.*, 2008, **176**, 1–12.
8. M. K. Rai, S. D Deshmukh, A. P. Ingle, A. K. Gade, *J. Appl. Microbiol.*, 2012, **112**, 841–852.
9. P. S. Schabes-Retchkiman, G. Canizal, R. Herrera-Becerra, *Opt. Mater.*, 2006, **29**, 95–99.
10. Z. Ahmad, R. Pandey, S. Sharma, *Ind. J. Chest. Dis. Allied. Sci*., 2006, **48**, 171–176.
11. P. Singh, H. Singh, Y. J. Kim, *Enzym. Microb. Technol.*, 2016, **86**, 75–83.
12. J. M. Nam, C. S. Thaxton, C. A. Mirkin, *Science*, 2003, **301**, 1884–1886.
13. W. J. Parak, D. Gerion, T. Pellegrino, *Nanotechnology*, 2003, **14**, R15.
14. A. Majdalawieh, M. C. Kanan, O. El-Kadri, *J. Nanosci. Nanotechnol.*, 2014, **14**, 4757–4780.
15. P. Singh, Y. J. Kim, H. Singh, *Int. J. Nanomed.*, 2015, **10**, 2567–2577.

16. H. Zazo, C. I. Colino, J. M. Lanao, *J. Control. Release,* 2016, **224**, 86–102.

17. N. Farhadian, R. U. Mashoof, S. Khanizadeh, Am. J. Orthod. Dentofac. Orthop. 2016, **149**, 155–160.

18. S. Prabhu, E. Poulose, *Int. Nano. Lett.*, 2012, **2**, 1–10.

19. K. Chaloupka, Y. Malam, A. M. Seifalian, *Trends Biotechnol.*, 2010, **28**, 580–588.

20. N. Nagasundaram, M. A. Rahuman, P. S. Raghavan, *Int. J. Pharm. Res. Bio–Sci.*, 2014, **3**, 153–164.

21. V. Lazar, *Anaerobe,* 2011, **17**, 280–285.

22. S. Periasamy, H. S. Joo, A. C. Duong, T. H. Bach, V. Y. Tan, S. S. Chatterjee, G. Y. Cheung, M. Otto, *Proc. Natl. Acad. Sci. USA*, 2012, **109**, 1281–1286.

23. D. Wu, W. Fan, A. Kishen, J. L. Gutmann, B. Fan, *J. Endod.*, 2014, **40**, 285–290.

24. L. A. Tamayo, P. A. Zapata, N. D. Vejar, M. I. Azocar, M. A. Gulppi, X. Zhou, G. E. Thompson, F. M. Rabagliati, M. A. Paez, *Mater. Sci. Eng. C Mater. Biol. Appl.*, 2014, **40**, 24–31.

25. S. Silver, *FEMS Microbiol. Rev.*, 2003, **27**, 341–353.

26. J. R. Morones, J. L. Elechiguerra, A. Camacho, K. Holt, J. B. Kouri, J. T. Ramirez, M. J. Yacaman, *Nanotechnology*, 2005, **16**, 2346–2353.

27. W. K. Jung, H. C. Koo, K. W. Kim, S. Shin, S. H. Kim, Y. H. Park, *Appl. Environ. Microbiol.*, 2008, **74**, 2171–2178.

28. N. R. Bury, C. M. Wood, *Am. J. Physiol.*, 1999, **277**, R1385–R1391.

29. S. Chernousova, M. Epple, *Angew. Chem. Int. Ed. Engl.*, 2013, **52**, 1636–1653.

30. M. Zhang, K. Zhang, B. De Gusseme, W. Verstraete, R. Field, *Biofouling*, 2014, **30**, 347–357.

31. M. J. Sweet, A. Chesser, I. Singleton, *Adv. Appl. Microbiol.*, 2012, **80**, 113–142.

32. S. Naraginti, A. Sivakumar, *Spectrochim. Acta A Mol. Biomol. Spectrosc*., 2014, **128**, 357–362.

33. S. Galdiero, A. Falanga, M. Vitiello, M. Cantisani, V. Marra, M. Galdiero, *Molecules*, 2011, **16**, 8894–8918.

34. S. L. Percival, P. G. Bowler, J. Dolman, *Int. Wound J*., 2007, **4**, 186-191.

35. S. Rajeshkumar, C. Malarkodi, K. Paulkumar, *J. Nanosci. Nanotechnol.*, 2013, **3**, 21–25.

36. D. D. Jurašin, M. Ćurlin, I. Capjak, T. Crnković, M. Lovrić, M. Babič, D. Horák, V. I. Vinković, S. Gajović, *Beilstein J. Nanotechnol.,* 2016 , **7**, 246-262.

37. V. K. Sharma, R. A. Yngard, Y. Lin, *Adv. Colloid Interface Sci.*, 2009, **145**, 83-96.

38. F. Zhao, D. Yao, R Guo, L. Deng, A. Dong, J. Zhang, *Nanomaterials,* 2015, **5**, 2054-2130.

39. J. Song, C. Yuan, T. Jiao, R. Xing, M. Yang, D. J. Adams, X. Yan, *Small*, 2020, **16**, 1907309.

40. D. M. Kirchmajer, R. Gorkin III, M. In het Panhuis, *J. Mater. Chem. B*, 2015, **3**, 4105-4117.

41. F. Ullah, M. B. H. Othman, F. Javed, Z. Ahmad, H. M. Akil, *Mater. Sci. Eng.CMater. Biol. Appl.*, 2015, **57**, 414-433.

42. L. S. Yap, M. C. Yang, *Colloids Surf. B.*, 2016, **146**, 204-211.

43. Y. Wang, L. Cao, S. Guan, G. Shi, Q. Luo, L. Miao, I. Thistlethwaite, Z. Huang, J. Xu, J. Liu, J. *Mater. Chem.,* 2012, **22**, 2575–2581; M. R. Reithofer, A. Lakshmanan, A. T. K. Ping, J. M. Chin, C. A. E. Hauser, *Biomaterials*, 2014, **35**, 7535–7542.

44. C. C. Piras, C. S. Mehon, D. K. Smith, *Chem. Eur. J*., 2020, **26**, 8452-8457.

45. E. M. Ahmed, *J. Adv. Res.*, 2015, **6**, 105-121.

46. E. Yadav, A. K. Khatana, S. Sebastian, M. K. Gupta, *New J. Chem.*, 2021, **45**, 415-422.

47. *(a)* A. Shome, S. Dutta, S. Maiti, P. K. Das, *Soft Matter*, 2011, **7**, 3011–3022; *(b)* Y. Wang, L. Cao, S. Guan, G. Shi, Q. Luo, L. Miao, I. Thistlethwaite, Z. Huang, J. Xu, J. Liu, J. *Mater. Chem.*, 2012, **22**, 2575–2581; *(c)* S. K. Mandal, S. Brahmachari, P. K. Das, *ChemPlusChem*, 2014, **79**, 1733–1746; *(d)* M. R. Reithofer, A. Lakshmanan, A. T. K. Ping, J. M. Chin, C. A. E. Hauser, *Biomaterials*, 2014, **35**, 7535–7542; *(e)* T. Simon, C.-S. Wu, J.-C. Liang, C. Cheng, F.-H. Ko, *New J. Chem.*, 2016, **40**, 2036–2043; *(f)* Y. Niu, T. Guo, X. Yuan, Y. Zhao, L. Ren, *Soft Matter*, 2018, **14**, 1227–1234; *(g)* F. Paladini, S. T. Meikle, I. R. Cooper, J. Lacey, V. Perugini, M. Santin, *J. Mater. Sci. Mater. Med.* 2013, **24**, 2461–2472; *(h)* J. Li, R. Xing, S. Bai, X. Yan, Soft *Matter*, 2019, **15**, 1704–1715.

48. P. Terech and R. G. Weiss, *Chem. Rev.*, 1997, **97**, 3133-3159.

49. *(a)* S. Murdan, B. Ven den Bergh, G. Gregoriadis, A. T. Florence, *J. Pharm. Sci.*, 1999, **88**, 615-619; *(b)* J. H. Van Esch, B. L. Feringa, *Angew Chem. Int. Ed. Engl.*, 2000, **39**, 2263-2266; *(c)* H. Willimann, P. Walde, P. L. Luisi, A. Gazzaniga, F. Stroppolo, *J. Pharm. Sci.*, 1992, **81**, 871-874.

50. Z. Wei, J. H. Yang, J. Zhou, F. Xu, M. Zrinyi, P. H. Dussault, Y. Osada, Y. M. Chen, *Chem. Soc. Rev.*, 2014, **43**, 8114-8131.

51. *(a)* A. R. Patel, P. S. Rajarethinem, A. Gredowska, O. Turhan, A. Lesaffer, W. H. De Vos, D. Van de Walle, K. Dewettinck, *Food Funct.*, 2014, **5**, 645-652; *(b)* A. R. Patel, N. Cludts, M. D. B. Sintang, A. Lesaffer, K. Dewettinck, *Food Funct.*, 2014, **5**, 2833-2841.

52. B. O. Okesola, D. K. Smith, *Chem. Soc. Rev.*, 2016, **45**, 4226-4251.

53. B. Behera, S. S. Sagiri, K. Pal, A. Srivastava, *J. Appl. Polym. Sci.*, 2013, **127**, 4910-4917.

54. W. L. Hinze, I. Uemasu, F. Dai, J. M. Braun, *Curr. Opin. Colloid Interface Sci.*, 1996, **1**, 502-513.

55. D. Subhashis, G. Vanitha, P. H.Bindu, M. NiranjanBabu, *Indian J. Biotech. Pharm. Res.*, 2014, **2**, 976-981.

56. *(a)* N. M. Sangeetha, U. Maitra, *Chem. Soc. Rev*., 2005, **34**, 821-836; *(b)* A. R. Hirst, B. Escuder, J. F. Miravet, D. K. Smith, *Angew. Chem. Int. Ed.,* 2008, **47,** 8002–8018; *Angew. Chem.,* 2008, **120,** 8122–8139; *(c)* X. Du, J. Zhou, J. Shi, B. Xu, *Chem. Rev*., 2015, **115,** 13165-13307; *(d)* B. O. Okesola, D. K. Smith, *Chem. Soc. Rev*., 2016, **45**, 4226–4251; *(e)* B. Hu, C. Owh, P. L. Chee, W. R. Leow, X. Liu, Y. L. Wu, P. Guo, X. J. Loh, X. Chen, *Chem. Soc. Rev*., 2018, **47,** 6917–6929; *(f)* D. K. Smith, *Molecular Gels: Structure and Dynamics* (Ed.: R. G. Weiss), Royal Society of Chemistry, Cambridge, 2018, 300–371.

57. P. R. A. Chivers, D. K. Smith, *Nat. Rev. Mater*., 2019, **4**, 463–478.

58. K. J. Skilling, F. Citossi, T. D. Bradshaw, M. Ashford, B. Kellam, M. Marlow, *Soft Matter*, 2014, **10**, 237 – 256.

59. *(a)* Q. Wei, M. Xu, C. Liao, Q. Wu, M. Liu, Y. Zhang, C. Wu, L. Cheng, Q. Wang, *Chem. Sci*., 2016, **7,** 2748–2752; *(b)* M. C. Nolan, A. M. Fuentes Caparros, B. Dietrich, M. Barrow, E. R. Cross, M. Bleuel, S. M. King, D. J. Adams, *Soft Matter*, 2017, **13**, 8426–8432.

60. *(a)* J. Eastoe, M. Snchez-Dominguez, P. Wyatt, R. K. Heenan, *Chem. Commun.*, 2004, 2608–2609; *(b)* J. J. D. de Jong, P. R. Hania, A. Pugzlys, L. N. Lucas, M. de Loos, R. M. Kellogg, B. L. Feringa, K. Duppen, J. H. van Esch, *Angew. Chem., Int. Ed.,* 2005, **44**, 2373– 2376; *Angew. Chem.,* 2005, **117**, 2425–2428; *(c)* S. Matsumoto, S. Yamaguchi, S. Ueno, H. Komatsu, M. Ikeda, K. Ishizuka, Y. Iko, K. V. Tabata, H. Aoki, S. Ito, H. Noji, I. Hamachi, *Chem. Eur. J.*, 2008, **14**, 3977–3986; *(d)* D. J. Cornwell, B. O. Okesola, D. K. Smith, *Angew. Chem. Int. Ed.,* 2014, **53**, 12461–12465; *Angew. Chem.*, 2014, **126**, 12669–12673; (*e*) E. R. Draper, E. G. B. Eden, T. O. McDonald, D. J. Adams, *Nat. Chem.*, 2015, **7**, 848–852; (*f*) D. J. Cornwell, O. J. Daubney, D. K. Smith, *J. Am. Chem. Soc.*, 2015, **137**, 15486–15492; (*g*) P. R. A. Chivers, D. K. Smith, *Chem. Sci.*, 2017, **8**, 7218–7227.

61. *(a)* R. J. Williams, A. M. Smith, R. Collins, N. Hodson, A. K. Das, R. V. Ulijn, *Nat. Nanotechnol.,* 2009, **4**, 19–24; *(b)* A. G. L. Olive, N. H. Abdullah, I. Ziemecka, E. Mendes, R. Eelkema, J. H. van Esch, *Angew. Chem. Int. Ed.,* 2014, **53**, 4132–4136; *Angew. Chem.,* 2014, **126**, 4216–4220; *(c)* K. E. Inostroza-Brito, E. Collin, O. Siton-Mendelson, K. H. Smith, A. Monge-Marcet, D. S. Ferreira, R. P. Rodriguez, M. Alonso, J. C. Rodriguez-Cabello, R. L. Reis, F. Sagus, L. Botto, R. Bitton, H. S. Azevedo, A. Mata, *Nat. Chem.,* 2015, **7**, 897–904; (*d*) J. R. Fores, M. L. M. Mendez, X. Mao, D. Wagner, M. Schmutz, M. Rabineau, P. Lavalle, P. Schaaf, F. Boulmedais, L. Jierry, *Angew. Chem. Int. Ed.,* 2017, **56**, 15984–15988; *Angew. Chem.,* 2017, **129**, 16200–16204.

62. J. Raeburn, B. Alston, J. Kroeger, T. O. McDonald, J. R. Howse, P. J. Cameron, D. J. Adams, *Mater. Horiz.,* 2014, **1**, 241–246.

63. *(a)* M. Lovrak, W. E. J. Hendriksen, C. Maity, S. Mytnyk, V. van Steijn, R. Eelkema, J. H. van Esch, *Nat. Commun.,* 2017, **8**, 15317; *(b)* J. Ruiz-Olles, D. K. Smith, *Chem. Sci.,* 2018, **9**, 5541–5550; *(c)* D. Spitzer, V. Marichez, G. J. M. Formon, P. Besenius, T. M. Hermans, *Angew. Chem. Int. Ed.,* 2018, **57**, 11349–11353; *Angew. Chem.,* 2018, **130**, 11519–11523.

64. *(a)* C. Felip-Leon, R. Cejudo-Marfn, M. Peris, F. Galindo, J. F. Miravet, *Langmuir,* 2017, **33**, 10322–10328; *(b)* A. Torres-Martinez, C. A. Angulo-Pachon, F. Galindo, J. F. Miravet, *Soft Matter,* 2019, **15**, 3565–3572.

65. L. E. Buerkle, S. J. Rowan, *Chem. Soc. Rev*., 2012, **41**, 6089–6102;

66. D. J. Cornwell, D. K. Smith, *Mater. Horiz*., 2015, **2**, 279–293.

67. *(a)* H. H. Tønnesen, J. Karlsen, *Drug Dev. Ind. Pharm.,* 2002, **28**, 621–630; *(b)* A. D. Augst, H. J. Kong, D. J. Mooney, *Macromol. Biosci.,* 2006, **6**, 623 – 633; *(c)* K. Y. Lee, D. J. Mooney, *Prog. Polym. Sci.,* 2012, **37**, 106–126.

68. B. B. Lee, P. Ravindra, E. S. Chan, *Chem. Eng. Technol.,* 2013, **36**, 1627–1642.

69. *(a)* G. Agrawal, R. Agrawal, *Small*, 2018, **14**, 1801724; *(b)* G. Agrawal, R. Agrawal, *Polymers* 2018, **10**, 418; *(c)* P. Kodlekere, A. Pich, *Chem. Nano. Mat.*, 2018, **4**, 889–896; *(d)* J. P. Newsom, K. A. Payne, M. D. Krebs, *Acta Biomater.*, 2019, **88**, 32-41; *(e)* Y. Wang, L. Guo, S. Dong, J. Cui, J. Hao, *Adv. Colloid Interface Sci.*, 2019, **266**, 1–20.

70. C. C. Piras, P. Slavik, D. K. Smith, *Angew.Chem. Int. Ed*., 2020, **59**, 853-859.

71. D. D. Jurašin, M. Ćurlin, I. Capjak, T. Crnković, M. Lovrić, M. Babič, D. Horák, V. I. Vinković, S. Gajović, *Beilstein J. Nanotechnol.*, 2016, **7**, 246-262.

72. *(a)* E. Torres, Y. N. Mata, M. L. Blazquez, J. A. MuÇoz, F. Gonzalez, A. Ballester, *Langmuir* 2005, **21**, 7951–7958; *(b)* J. Yang, H. Zheng, S. Han, Z. Jiang, X. Chen, *RSC Adv.*, 2015, **5**, 2378-2382; *(c)* S. V. Kapranov, V. I. Ryabushko, *J. Nanopart. Res*., 2018, **20**, e275; *(d)* Y. Shao, C. Wu, T. Wu, C. Yuan, S. Chen, T. Ding, X. Ye, Y. Hu, *Int. J. Biol. Macromol.*, 2018, **111**, 1281–1292.

73. *(a)* M. Omidkhoda, N. Hasanzadeh, F. Soleimani, H. Shafaee, *J. Dent. Res.*, 2019, **16**, 372–376; *(b)* J. Stojkovska, Z. Djurdjevic, I. Jancic, B. Bufan, M. Milenkovic, R. Jankovic, V. Miskovic-Stankovic, B. Obradovic, *J. Biomater. Appl.*, 2018, **32**, 1197–1211; *(c)* H. Zhang, M. Peng, T. Cheng, P. Zhao, L. Qiu, J. Zhou, G. Lu, J. Chen, *J. Mater. Sci.*, 2018, **53**, 14944-14952.

74. *(a)* J. Nanda, A. Biswas, B. Adhikari, A. Banerjee, *Angew. Chem. Int. Ed.*, 2013, **52**, 5041–5045 *Angew. Chem*., 2013, **125**, 5145-5149; *(b)* P. Thoniyot, M. J. Tan, A. A. Karim, D. J. Young, X. J. Loh, *Adv. Sci.* 2015, **2**, 1400010; *(c)* S. Grijalvo, R. Eritja, D. D. Díaz, *Gels*, 2019, **5**, 24.

75. P. Terech, D. Pasquier, V. Bordas, C. Rossat, *Langmuir*, 2000, **16**, 4485–4494.

76. D. J. Mercurio, R. J. Spontak, *J. Phy. Chem. B.*, 2001, **105**, 2091–2098.

77. L. Le Le Pluart, J. Duchet, H. Sautereau, P. Halley, J-F Gerard, *Appl. Clay Sci.*, 2004, **25**, 207–219.

78. P. F. Lim, X. Y. Liu, L. Kang, P. C. Ho, S. Y. Chan, *Int. J. Pharm.*, 2008, **358**, 102–107.

79. M. I. Silva, A. I. Barbosa, S. A. Costa Lima, P. Costa, T. Torres, S. Reis, *Nanomaterials*, 2020, **10**, 986.

80. G. P. Andrews, D. S. Jones, *Biomacromolecules.*, 2006, **7**, 899–906.

81. J. Du, H. Sing, T. H. Yi, *Artif. Cells. Nanomed. Biotechnol.*, 2017, **45**, 211–217.

82. C. Wang, Y. J. Kim, P. Singh, *Nanomed. Biotechnol.*, 2016, **44**, 1127–1132.